

THE DESIGN AND DEVELOPMENT OF A
HUMAN-POWERED AIRPLANE

A THESIS

Presented to
the Faculty of the Graduate Division

by

James Marion McAvoy, Jr.

In Partial Fulfillment
of the Requirements for the Degree
Master of Science in Aerospace Engineering

Georgia Institute of Technology

June, 1963

3.4
12B

THE DESIGN AND DEVELOPMENT OF A
HUMAN-POWERED AIRPLANE

Approved:

Date Approved by Chairman:

May 27, 1963

In presenting the dissertation as a partial fulfillment of the requirements for an advanced degree from the Georgia Institute of Technology, I agree that the Library of the Institution shall make it available for inspection and circulation in accordance with its regulations governing materials of this type. I agree that permission to copy from, or to publish from, this dissertation may be granted by the professor under whose direction it was written, or, in his absence, by the dean of the Graduate Division when such copying or publication is solely for scholarly purposes and does not involve potential financial gain. It is understood that any copying from, or publication of, this dissertation which involves potential financial gain will not be allowed without written permission.

ACKNOWLEDGMENTS

The author wishes to express his most sincere appreciation to Professor John J. Harper for acting as thesis advisor, and for his ready advice at all times.

Thanks are due also to Doctor Robin B. Gray and Doctor Thomas W. Jackson for serving on the reading committee and for their help and advice.

Gratitude is also extended to all those people who aided in the construction of the MPA and to those who provided moral and physical support for the project. Among these are Professor Donnell W. Dutton, Mr. George W. D. Cook, Mr. Dewey L. Ransom, Mr. John A. Ellis, Mr. David A. Shelton, Mr. Royce N. Hall, Mr. Robert W. Ritchie, and Mr. David R. Fern.

The author further wishes to acknowledge the material aid furnished by The Du Pont Company, Lockheed Aircraft Company of Georgia, and the Shell Chemical Corporation.

Last, but not least, the author sincerely acknowledges the help of his patient wife who typed the rough draft and who helped with the construction.

TABLE OF CONTENTS

	Page
ACKNOWLEDGMENTS	ii
LIST OF FIGURES	iv
LIST OF TABLES	vi
LIST OF SYMBOLS	vii
SUMMARY	ix
CHAPTER	
I. INTRODUCTION	1
II. DESIGN ANALYSIS	4
General Considerations	
Preliminary Design	
Propulsion System	
Stability and Control Analysis	
III. RESULTS	17
IV. CONCLUSIONS AND RECOMMENDATIONS	21
REFERENCES	24
APPENDICES	25

LIST OF FIGURES

Figure	Page
1. Dimensional Data for MPA	19
2. Drag Polars for Four Configurations Tested	30
3. Profile Drag Polar for Constant Chord Wing Operating Out of Ground Effect	31
4. Wing Spars	34
5. Balsa Wood Rib Section	35
6. Ribs and Spars Joined Together	36
7a. Completed Wings Before Assembly to Aircraft	37
7b. Wing Internal Structures	38
7c. Wing Section Showing Aileron	39
7d. Airplane Left Side View During Final Assembly	40
7e. Airplane Front View After Final Assembly	41
8a. Fuselage Front View	43
8b. Side View of Fuselage and Shroud	44
9a. Front Propeller During Construction	45
9b. Top View of Shroud While Jigged During Construction	46
9c. Side View of Shroud During Construction	47
9d. Rear View of Shroud and Propellers After Assembly to Aircraft	48
9e. Propeller Hub and Front Shroud Mounting Struts	49
10. Camber Effect on the Section Minimum Drag Coefficient of Thick NACA Laminar Flow Airfoils at a Constant Reynolds Number as Taken from the NACA Data	52
11. Section Drag Characteristics of the NACA 65 ₂ 418 Airfoil Taken from the War Time Report ACR Number L4HLL	53

Figure	Page
12a. Top View of Buckled Spar Cap	59
12b. Front View of Buckled Spar Cap	60
12c. Rear View of Buckled Spar Cap	61
13. Horsepower-Endurance Chart for a One Hundred and Sixty Pound Man	72

LIST OF TABLES

Table	Page
1. Propeller Section Data	67
2. Shroud Mean Camber Line	69

LIST OF SYMBOLS

A_{wa}	Area of wing spanned by an aileron
AR	Aspect-ratio, b^2/S
b	Wing span
C_D	Airplane drag coefficient
C_f	Airplane skin friction drag
C_{Df}	Fuselage drag coefficient based on fuselage wetted area
C_L	Wing lift coefficient
D	Drag
H	Horsepower, $\frac{TV}{550}$
h	Altitude
L	Lift
M	Wing bending moment due to actual loads
m	Wing bending moment due to a one-pound vertical load at the tip
m.a.c.	Mean aerodynamic chord
P	Roll velocity
P_{cr}	Euler column buckling load
q	Dynamic pressure
R	Propeller radius
r	Blade station measured from center of propeller
S	Wing planform area
T	Propeller thrust
V	Velocity of resultant wind
W	Weight

y	Station along wing semi-span
z	Height of tip plate

Subscripts

a	Aileron
e	Effective
f	Fuselage
g	Geometric
int	Interference
sh	Shroud
tp	Tip plate
w	Wing

Greek Symbols

Γ	Blade bound vortex strength
γ	Propeller induced
Δ	Indicates increment of change
δ	Correction factor between ideal (elliptic) and true lift distributions
η	Non-dimensional semi-span position, $\frac{2y}{b}$
η_p	Propeller efficiency
τ	Aileron effectiveness
ϕ	Angle between propeller blade resultant velocity and propeller disk
ψ	Volume flow through propeller

SUMMARY

An aircraft operated by muscle power alone is proposed in this report; many attempts have been made by man to fly by his muscles alone but most have resulted in failure.

The design incorporates some unique features, including shrouded-counter-rotating propellers mounted at the tail of the plane. The shroud thus replaces the conventional tail surfaces, while improving propeller efficiency at the same time. A low wing configuration with wing tip plates is used to provide maximum aerodynamic efficiency. Ultra light-weight construction is used throughout to obtain the lightest possible design.

A stability and control analysis indicates adequate control power and adequate static stability about all three axes.

An investigation of performance characteristics shows that at a flight speed of 20 miles per hour about .50 horsepower is required. Take-off velocity is 17 miles per hour. It was determined that a human being can produce at least .7 horsepower in short spurts, and a steady .5 horsepower for six minutes.

It is concluded that the design is possible, and that man-powered flights are possible with this aircraft.

CHAPTER I

INTRODUCTION

One of man's earliest dreams was to be able to sustain himself in the air by his own power. This dream is recorded in many ways. For example, there were many legendary figures, some mythical and some who actually lived, that were reported to have been able to fly. However, there is no evidence to support the claims that these people could fly and there is no sound reasoning as to why they could have flown.

Proceeding from legend to history, men began to apply reasoning to their attempts to fly. The understanding of the fundamentals of bird flight was undertaken with much zeal but little success. It is found that the wing loading for most birds that sustain flight for long periods of time is, at the most, only slightly more than one pound per square foot. Birds with larger wing loadings are limited to flights of smaller duration. Early attempts at flight by human power were made with pairs of arm-operated flapping wings, as it was desired to duplicate bird flight. However, wing loading was invariably too great for such flights to be successful.

There was much interest in Germany, even as late as the mid 1930's, in developing a muscle-powered aircraft of the flapping wing configuration. There is no known successful flight of anyone that used this configuration.

At the same time that the Germans were attempting to develop a man-powered flapping wing aircraft, there was much interest in man-

powered flights throughout all of Europe. Many of the European governments were offering prizes to stimulate interest in the development of human-powered aircraft. One of the most successful flights of this period was made in Italy in 1936 by Enea Bossi in a high-wing monoplane that was pedal powered.

Although Bossi was not able to take off, he was able to fly one thousand meters without the aids of winds or thermals after having been launched at an altitude of less than 25 feet. This flight represented a considerable improvement over the flight that any glider could have made under the same flight conditions, since the glide ratio of the most efficient gliders known has not been much greater than 40 to 1. However, Bossi's aircraft left much to be desired as a human powered aircraft, since it could not take off by the use of the pilot's muscles alone. The first man-powered craft to leave the ground unaided was made in November, 1961, in England by a group at the South Hampton University. The longest flight known was made in May, 1962, in England by a group at the de Havilland Aeronautical Technical School. This aircraft was piloted by John Winnpenny. He was able to fly slightly over one-half of a mile at an altitude under ten feet.

Flights such as the ones noted above definitely show that to some extent man is able to fly by using his own strength. However, it is felt that both the range and maximum altitude obtainable by human-powered aircraft can be extended beyond one mile and ten feet, respectively.

A human-powered aircraft must, by necessity, be ultra light and fly at very low speeds. Therefore, the design of a human-powered airplane would require an investigation and study of the practical applica-

tion of incompressible aerodynamics at very low Reynolds numbers. Unfortunately, information in the literature concerning aerodynamic phenomena at very low Reynolds numbers is so widely scattered that it is difficult to collect and correlate. The structural problem is made more difficult because, in this case, one strives not for the lightest practical design but for the lightest possible design.

CHAPTER II

DESIGN ANALYSIS

General Considerations

The design conditions to be met are as follows:

1. The design should be such that a man weighing 185 pounds who is in good physical condition could make continuous flights for distances in excess of one mile while obtaining an altitude of, or exceeding, ten feet for at least fifty per cent of the flight.
2. Only very low wind velocities (five mph or less) and no thermal current effects can be tolerated on a performance test of the aircraft.
3. No external help can be obtained for take-off nor will any energy storing devices be allowed in the aircraft.
4. The aircraft should be maneuverable such that it could execute the turns necessary to fly a figure "8" course not exceeding one mile in length.
5. The stresses in the structure must be less than the yield or buckling load for a load-factor of 1.125. All loads calculated for an altitude of one thousand feet in standard air.

Preliminary Design

The initial step in the investigation was to estimate weights for the various components of the airplane (including the weight of the pilot). Then the aerodynamic relations for lift and drag were used with

the formula for horsepower (in terms of thrust and velocity) to find a suitable wing configuration for the weight assumed.

To satisfy the equation of equilibrium of the forces on the airplane, the lift was set equal to the gross weight and the thrust equal to the estimated drag:

$$W = L = C_L q S$$

$$T = D = C_{Dq} S$$

$$H_{req} = \frac{TV}{550}$$

The configuration thus found was used to compute a new weight estimate for the wing designed to satisfy design condition five. Due to structural limitations, the best wing configuration is not necessarily the one requiring the least horsepower, i.e. for a given amount of surface area a long slender wing would cause less drag than a short wing, but the long slender wing would require a larger amount of material in the wing spars to withstand the greater stresses arising from the larger bending moment on the wing.

In order to obtain a wing configuration, it was necessary to assume two of the three parameters in the lift equation. The third parameter was solved for in terms of the two assumed parameters and the gross weight. An airfoil was then selected for which the value of C_{Dow} could be obtained from the literature and for which the induced drag coefficient was

$$C_{Di} = \frac{C_L^2 (1 + \delta)}{AR} \quad (\text{Reference 1}).$$

Further, C_{Dof} was estimated to be 30 per cent of C_{Dow} (based on a comparison of the wetted areas of the wing and fuselage, neglecting Reynolds' number effect on the fuselage).

After estimating the drag coefficient,

$$C_D = C_{Dow} + C_{Df} + \frac{C_L^2 (1 + \delta)}{\pi AR},$$

a value for thrust required was computed, thus allowing the horsepower required to be found.

In order to minimize the weight of the wing, various structural materials were considered and their properties compared in conjunction with various rib and spar configurations. It was finally decided that aluminum, balsa wood, and Mylar¹ would be used throughout the aircraft (see Appendix I). The ribs are made of balsa and the spars are made of aluminum while the wing is covered with Mylar.

With wing weight established, the airplane weight was estimated to be approximately 110 pounds (the materials selected also allowed a more accurate estimate of fuselage weight which was below the original estimate). However, it was found that a very high lift coefficient ($C_L = 0.9$) must be maintained with a forward speed of approximately 22 mph to keep the horsepower required low (below one horsepower).

It became apparent that some method was needed to reduce the induced drag which would be large due to the high value of C_L required for flight.

¹Mylar is a polyester plastic film produced by the E. I. Du Pont De Nemours and Company, Wilmington, Delaware.

At least two methods are known to reduce the induced drag: keep the wing as close to the ground as possible to make the most effective use of the ground to reduce the downwash behind the wing; and use end plates as "fences" on the wing tips to reduce the effect of the tip vortices (or tip spillage).

The resultant effect of the two above methods is to increase the effective aspect-ratio, thus decreasing the induced drag.

The changes in effective aspect-ratio are:

1. Due to ground effect,

$$\frac{\Delta AR}{AR_g} = 0.09 \frac{b}{h} \text{ (reference 2).}$$

2. Due to tip plates,

$$\frac{\Delta AR}{AR_g} = 1.9 \frac{z}{b} \text{ (reference 2).}$$

However, these were empirical formulas based on flight conditions at Reynolds numbers from three to four times greater than the Reynolds numbers to be encountered by the wing configuration found above. Therefore, tests were run in the Georgia Tech 30-inch wind tunnel to determine if the formulas were applicable at the lower Reynolds number. The test data showed that the formulas could not only be used, but were actually slightly conservative (see Appendix II).

Using the above methods for increasing the effective aspect-ratio and further setting the wing taper ratio at 2 1/2:1 (to give the smallest in the expression for induced drag), the last iteration for the wing configuration is as follows:

Step 1 Substitute the assumed weights from the previous iteration (see Appendix III) into the lift equation.

Weights: Pilot	185 lbs.
Fuselage and cockpit	25 lbs.
Prop and drive	25 lbs.
Wing	50 lbs.
<hr/>	
Total	285 lbs.

$$W = C_L q s = 285 \text{ lbs.}$$

Step 2 Assume two parameters from the lift equation:

$$C_L = 0.9 \quad (\text{see Appendix IV})$$

$$S = 287 \text{ ft.}^2$$

From the lift equation,

$$q = \frac{285}{(.9)(287)} = 1.102 \text{ lbs./ft.}^2$$

Thus, the corresponding velocity is

$$V^2 = \frac{1.102}{(1/2)(.002308)} = 956 \text{ ft.}^2/\text{sec.}^2$$

$$V = 30.8 \text{ ft./sec.}$$

Step 3 A wing span of 54 feet was chosen, and an internal structure was selected (see Appendix III) consisting of balsa wood rib sections every twelve inches and two truss type aluminum spars. The wing weight was computed and found to check very closely with the assumed weight. A stress analy-

sis showed that the structure was adequate to satisfy the design conditions (see Appendix V).

Step 4 Compute the geometric aspect-ratio and correct for ground effect and end plating.

$$AR_g = \frac{(54)^2}{287} = 10.15$$

Due to ground effect at ten feet altitude:

$$\Delta AR = (10.15)(.09)(54)/10 = 4.93$$

Due to end plates 30 inches high:

$$\Delta AR = (10.15)(1.9)\frac{(2.5)}{54} = 0.89$$

The effective aspect ratio then becomes

$$AR_e = 15.97$$

for which

$$\delta = 0.03 \text{ (reference 1)}$$

Step 5 Estimate the profile drag coefficient and compute the horsepower required for the flight velocity at ten feet of altitude.

$$C_{Do} = C_{Dow} + C_{Dof} + C_{Do_{tp}} + C_{Do^{sh}} + C_{Do_{int}}$$

$$R_n = 1.31 \times 10^6$$

$$C_{Dow} = 0.008 \text{ (see Appendix IV)}$$

$$C_{Dof} = 0.0011$$

$$C_{Dotp} = 0.0008$$

$$C_{Doint} = 0.0002 \text{ (see Appendix VII)}$$

$$C_{Dosh} = 0.0016$$

$$C_{Do} = .012$$

$$C_L = 0.9 \text{ (see Step 2)}$$

$$C_D = C_{Do} + \frac{(0.81)(1 + 0.03)}{\pi(15.97)} = 0.029$$

$$D = (0.029)(1.102)(287) = 9.18 \text{ lbs.}$$

$$H_{req} = \frac{(9.18)(30.8)}{550} = 0.515$$

Propulsion System

The propellers are the counter-rotating pusher type with a shroud. The front propeller has four blades, and the rear propeller has three blades (the difference in numbers of blades per propeller is to insure that the front and rear blades do not match up to give a forced vibration with a frequency that is an integer multiple of the drive shaft velocity).

This configuration was chosen for several reasons. Tractor propellers were not practical due to the low wing configuration, since they would require pylons on the wings to mount them. Further, a single tractor prop mounted in front of the fuselage would have caused much

higher velocities and turbulent flow over the fuselage, which would increase the fuselage drag. The pusher configuration only slightly affects the flow over the fuselage, and could be mounted directly on the rear end of the empennage with no pylon extending into the air stream. This arrangement requires only a simple torque tube device for a drive-shaft from the cockpit. The shroud was added with almost no increase in drag over the drag that would be encountered by a conventional tail configuration consisting of vertical and horizontal stabilizers, since the wetted areas of the two types of tail configurations would be almost the same. Furthermore, the trailing edge of the shroud was hinged in four places to give control surfaces consisting of two elevators and two rudders. The shroud tends to reduce the blade-tip vortices and make the propeller more efficient. The propellers were made counter-rotating to eliminate the losses encountered due to the rotation imparted to the wake by a single propeller. Thus, the overall result is to increase the propeller efficiency while introducing almost no adverse effects.

The propeller was designed using a method combining momentum and blade element theory, while the shroud was designed by the method of singularities (see reference 4).

The design data and a brief outline of the propeller and shroud designs are contained in Appendix VII.

Stability and Control Analysis

Primarily, the stability and control analysis must be done to determine if there is enough control power to correct for slight deviations from the normal flight positions (assuming very calm weather conditions).

The requirement for lateral control is that there exist enough

aileron power to correct for the rolling moment due to any dihedral effect from any cross wind that might be encountered in a full turn. Furthermore, due to the close proximity of the ground the terminal roll velocity must be computed to insure that it can not exceed 12 degrees per second for a 15 degree aileron deflection.

The safety of the plane is of utmost importance. Thus, a cross wind at least three times as strong as the maximum allowable wind for flight test purposes (design condition 2) will be used for dihedral effect calculations. The maximum effective dihedral (due to bending deflections) is six degrees.

The changes in lift due to a 15 mile-per-hour cross wind are found along the two semi-spans and the moments due to the changes in lift are summed to find the resulting rolling moment on the airplane.

The resultant restoring moment from the ailerons at full deflection is found by determining the change in lift over the wing due to the deflection of the aileron. Two-dimensional airfoil theory for a flapped airfoil was used to determine the change in lift. However, the two-dimensional values must be corrected to account for the loss in effectiveness of the ailerons near their ends, where there is considerable spillage of the flow around the ends when the ailerons are deflected.

The change in lift on the wings due to aileron deflection is found by determining the change in the lift coefficient over the wing ahead of the ailerons and basing the resultant change in lift on the area spanned by the ailerons (the wing has a straight 50 per cent chord line).

The change in lift coefficient for a 15 degree deflection of a

plain flap is $\Delta C_L = 0.3$ (reference 5) and the span correction factor is 0.9 (reference 6).

From the wing geometry the area of the wing spanned by the ailerons is

$$A_{wa} = 88 \text{ ft.}^2$$

Thus, the change in lift is

$$L = (0.4)(1.102)(88)(0.9) = 26 \text{ lbs.}$$

The resultant moment arm for the change in lift on the wings is approximately 6 feet. Thus, the resultant restoring moment for the above unbalanced condition is approximately 156 foot-pounds. The maximum rolling moment from the dihedral effect is only 25 foot-pounds.

The terminal roll velocity is

$$P = \frac{2V}{b} \frac{.9}{57.3} \frac{(\tau_2^3 - \tau_1^3)(1 - TR) + 3TR(\tau_2^2 - \tau_1^2)}{TR + 3} \quad (\text{reference 6}).$$

where

$$\tau = .45 \quad (\text{reference 6})$$

$$\delta_a = 15^\circ$$

$$\tau_1 = .148$$

$$\tau_2 = .407$$

The terminal roll velocity due to maximum aileron deflection is

one half of a degree per second which should give the pilot enough time to recognize an unbalanced rolling condition and correct for it before getting too close to the ground.

Furthermore, when one wing tip approaches the ground during a roll, the downwash behind the semi-span closest to the ground is reduced. This in turn reduces the induced angle of attack, which increases the effective angle of attack and causes more lift on the lower wing. This in turn tends to give a rolling moment helping correct the adverse condition.

Enough elevator power must be available to trim the airplane in pitch under all flight conditions. An investigation of the airplane's aerodynamic pitching moment and static unbalance revealed that the center of gravity location with respect to the wing center of lift was very critical, and that the unbalance due to aerodynamic pitching moment was negligible compared to the unbalanced condition that would exist if the center of gravity and center of lift were separated by more than four inches, i.e. the longitudinal c.g. travel must be less than four inches on either side of the 41 per cent chord of the wing. The maximum pitching moment caused by the maximum allowable unbalance would be plus or minus 95 foot-pounds. The airfoil selected for use on the aircraft does not exhibit a tendency to pitch about its 41 per cent chord at the design lift coefficient, as this is the theoretical center of pressure. Every effort must be made to locate the center of gravity so that it coincides very nearly with the center of lift.

The elevator power is determined by assuming that the shroud cross-section is an 0006 NACA airfoil, with two trailing edge strips

pivoted to deflect as an elevator with maximum deflections of 20 degrees upward and 20 degrees downward. The elevator is pivoted three inches behind the elevator leading edge. The chord and span of the elevator are 18 inches and 20 inches, respectively.

It was further assumed that any change in angle of attack on the shroud "airfoil" due to an elevator deflection is equal to the change in the slope of a line drawn through the leading edge of the shroud and the trailing edge of the elevator. Also, it is assumed that the wind velocity is the average of the velocities along the inner and outer surfaces of the shroud.

The force caused by a maximum deflection computed from airfoil theory is 9.4 pounds. Since the quarter chord of the shroud is located 11 feet behind the wing 41 per cent chord, the elevator is capable of providing a maximum pitching moment of 104 foot-pounds at full deflection which exceeds the minimum amount required.

Due to symmetry of the aircraft and the calm weather conditions required for flight, the requirements for rudder power will not be critical. The rudders are constructed the same way as the elevators, but are somewhat smaller.

The restoring moment caused by the maximum deflection of the rudders is approximately plus or minus 40 foot-pounds. This restoring moment must be large enough to overcome any adverse yaw caused by the maximum deflection of the aileron.

The coefficient of the adverse yawing moment caused by a rolling wing may be estimated by the following formula,

$$C_n = \frac{C_L}{8} \frac{Pb}{2V} \text{ (reference 6)}$$

The value thus obtained from this formula is $C_n = 0.0009$.

The adverse yawing moment is found from the formula,

$$N = C_n qSb$$

$$N = (0.0009)(1.1)(287)(54) = 15 \text{ ft. lbs.}$$

CHAPTER III

RESULTS

This investigation illustrates the fact that with new ultra light materials for construction, man should be able to sustain flight by his own strength for periods sufficiently long to fly distances exceeding one mile. Over level terrain and flying only three or four feet above the ground, continuous flights lasting up to twenty minutes are possible. At 10 feet above the ground continuous flights of approximately one and one-half miles are possible over level ground.

The airplane will take off at an air speed of approximately 17 mph with a wing lift coefficient of approximately $C_L = 1.2$. Then speed may be gained so that the lift coefficient can be reduced to $C_L = 0.9$ which is the value of the design lift coefficient of the airfoil. The design lift coefficient will be realized when the airspeed is 20 mph, which is the design cruise velocity.

The profile drag coefficient for the airplane is $C_D = 0.012$. Thus, the minimum horsepower required for cruise at the design velocity and lift coefficient is $H = 0.515$ for 100 per cent efficient propellers. The effective Reynolds number of the propeller at the blade stations three-fourths of the blade length from the center of the propeller is approximately $Rn = 200,000$. Due to the low Reynolds number, it is difficult to determine the exact efficiency of the propeller, but the propeller and drive were estimated to be 85 per cent efficient. This is felt to be slightly conservative since the drag of the shroud is in-

cluded in the drag of the airplane rather than being included in the efficiency of the propulsion system as is customary. The total horsepower required for level flight at ten feet above the ground is $H = 0.6$.

The investigation of the controllability of the airplane shows that the airplane should be stable and readily controllable. However, since the wing span is so large and the flights must take place very close to the ground, it will probably be difficult to fly a figure "8" course in one continuous flight as the minimum radius of turn will probably be so great that the total path to be traveled while performing this maneuver will require time exceeding the endurance of the pilot.

The major geometric and physical features are as follows:

Empty weight	110 pounds
Wing span	54 feet
Length	16 feet
Taper ratio	2 1/2:1
Wing area	287 square feet
Wing airfoil	NACA 65 ₂ 915
Propeller diameter	7 feet
Shroud outer diameter	7 1/2 feet

The MPA (man powered airplane) should meet all of the design requirements except design condition four as a path exceeding one mile will probably be needed to execute the figure "8" turns. Dimensional data and external arrangements of the MPA are shown in Figure 1.

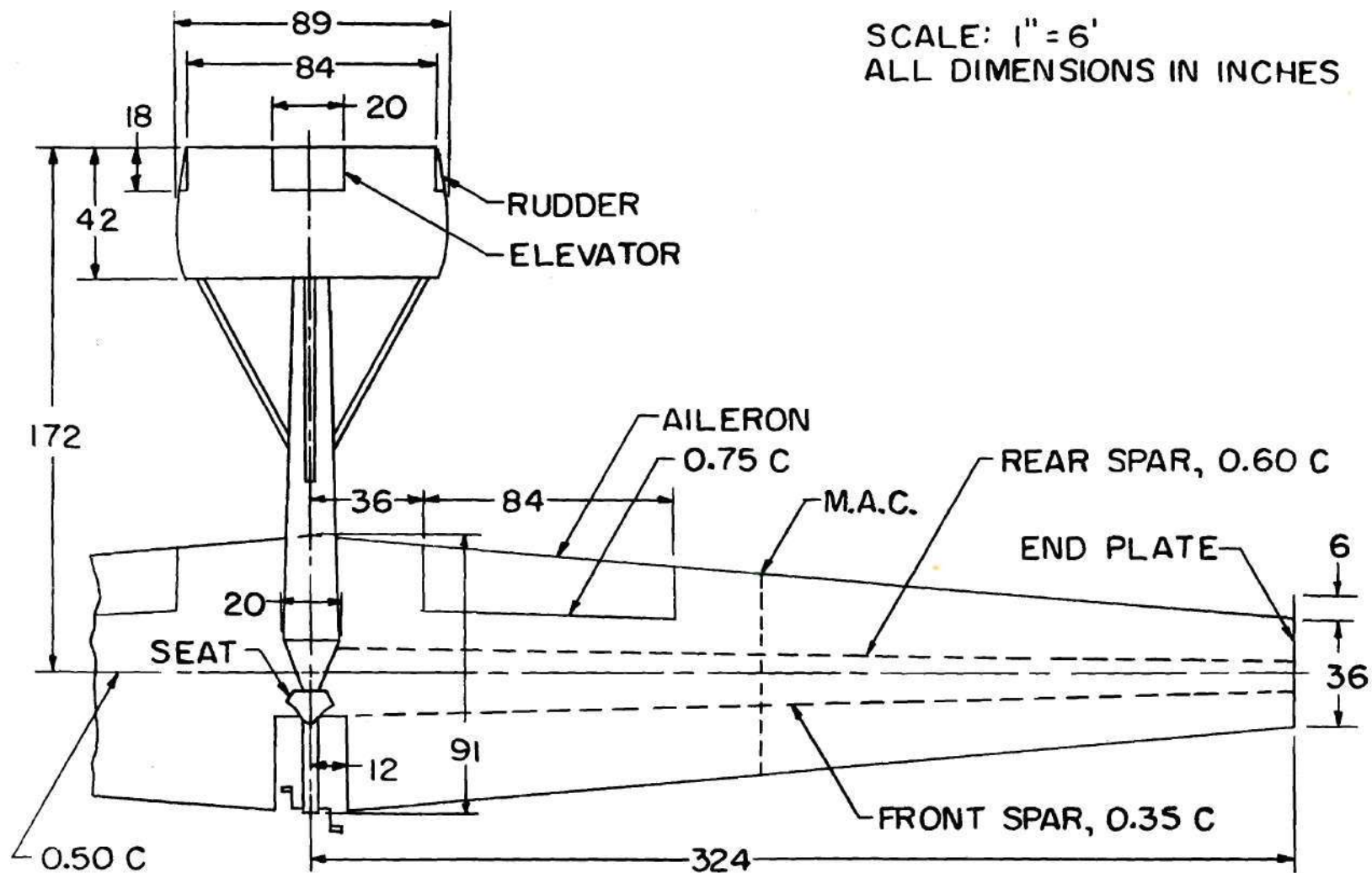


Fig. 1 Dimensional Data for MPA

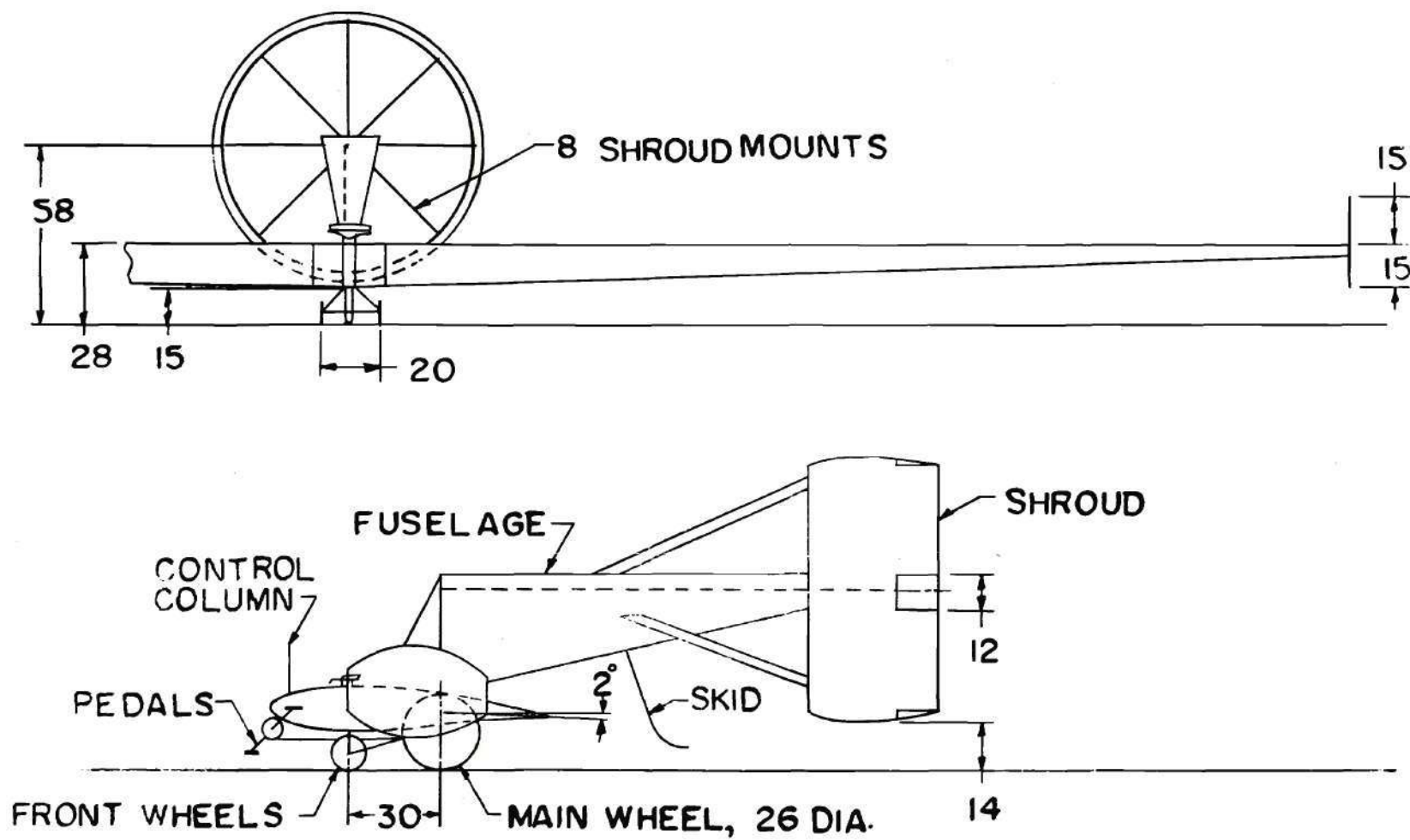


Fig. 1 (Continued) Dimensional Data for MPA

CHAPTER IV

CONCLUSIONS AND RECOMMENDATIONS

The general construction methods used on the airplane were satisfactory. The general wing construction could be improved very little and still provide as light a structure as possible that would be strong enough. In the early stages of construction it was felt that the wing would not be rigid enough in torsion, and as a safety measure a cable was added along the bottom spar cap of the front spar which could be used to deform the wing so as to reduce the pitch if the wing showed tendencies to diverge in pitch. However, after applying the skin it was found that the wing was sufficiently rigid to perform as desired. Further, the center of gravity, the center of pressure, and the center of shear for any wing cross section was found to be separated by not more than one per cent of the section chord, except for the portion of the wing from the centerline of the plane out to the first rib. Thus, there is very little twist along the wing due to torsion. However, on the first attempt to get the plane airborne, the top spar caps on the right wing buckled between the root and the first rib. It appears that this was caused because the wing twisted over this section so that the compression load acted on a "curved" spar cap rather than the initially straight spar cap. The twist probably caused a local buckling or wrinkling of the flange on the spar cap "T" section and consequently lowered the critical buckling load below the load that was experienced by the spar cap.

Difficulties were encountered in maintaining the shroud cylindrical. However, this difficulty was overcome by adding a spar made of pine to the structure. Since it is necessary to get the maximum efficiency for the propulsion system for a man-powered aircraft, the use of the shroud is justified on such a craft.

The design weights were met on every component of the airplane except for the fuselage which went nearly twenty-five pounds overweight. This difficulty was encountered because the materials on hand were used in order to speed up the construction rather than design the fuselage for lighter materials. The weight of the fuselage construction could have been reduced at least 20 pounds by using magnesium rather than aluminum throughout the fuselage without sacrificing strength.

Some difficulty was experienced in holding the balsa wood construction to design specifications, but the errors of construction do not seem to subtract significantly from the aerodynamic characteristics of the wings.

The wing structure would be stronger if the spar caps had been formed from continuous members rather than making joints in the spars, but the spar caps would be much more difficult to form.

The aerodynamic design of the airplane appears to be excellent and there is little or no recommended change. However, since the wing can be made sufficiently rigid in torsion by properly applying the skin, some improvement in the performance of the airplane could be gained by increasing the wing span to 60 feet. This would reduce the induced drag and increase the maximum altitude obtainable with very little effect on the maneuverability of the airplane. A wing longer than 60 feet would

encounter considerable torsional deflection and would be very hard to turn. Besides the difficulty in banking enough to turn, it is expected that the wing tip on the inside of a turn would be susceptible to a decrease in lift as the resultant airspeed would decrease with a large rate of yaw.

The magnitude of the problem of building a man-powered airplane becomes evident when one considers that a conventional airplane carries only about 50 pounds per horsepower available, whereas the man-powered aircraft must carry approximately 500 pounds per horsepower available. Because of this condition there can be very little margin of safety in any of the structure and in many cases the parts must operate very near their ultimate load--this is particularly true of the drive system. Thus, much difficulty with the operation of the craft can be expected unless great care is taken in the starting of the runs and accelerations so that the ultimate loads are not exceeded. Also, the airplane must be restricted to flight in extremely calm weather.

REFERENCES

1. Pope, Allan, Basic Wing and Airfoil Theory, McGraw-Hill Book Company, Inc., New York, 1951.
2. Hoerner, S. F., Fluid-Dynamic Drag, Published by the author, Midland Park, New Jersey, 1958.
3. Jacobs, Eastman W., Preliminary Report on Laminar Flow Airfoil and Boundary Layer Investigations, NACA WL-345, U.S. Government Printing Office, Washington, D. C., 1939.
4. Castles and Gray, An Investigation of an Approach to the Problem of Determining the Optimum Design of Shrouded Propellers, Engineering Experiment Station, Georgia Institute of Technology, Atlanta, Georgia, 1960.
5. Albert and Von Doenhoff, Theory of Wing Sections, Dover Publications, Inc., New York, 1959.
6. Perkins and Hage, Airplane Performance Stability and Control, John Wiley and Sons, Inc., New York, 1960.
7. Kohn, Jean, Properties and Uses of Balsa, Balsa Ecuador Lumber Corp., New York, 1957.

APPENDICES

APPENDIX I

STRUCTURAL MATERIALS AND THEIR PROPERTIES

Material:

1. Aluminum--2024S-T

Modulus of Elasticity.....	10,300,000 psi.
Tensile Yield Strength.....	48,000 psi.
Density.....	175 lbs./cu. ft.

2. Balsa Wood¹

a. Grade I

Modulus of Elasticity.....	300,000 psi.
Tensile Yield Strength....	1,375 psi.
Density.....	6 lbs./cu. ft.

b. Grade II

Modulus of Elasticity.....	600,000 psi.
Tensile Yield Strength....	3,050 psi.
Density.....	11 lbs./cu. ft.

c. Grade III

Modulus of Elasticity.....	900,000 psi.
Tensile Yield Strength....	4,525 psi.
Density.....	15 1/2 lbs./cu. ft.

3. Mylar--60 Gauge

Tensile Yield Strength.....	20,000 psi.
Density.....	25 sq. yds./lb.
Heat Shrinkable-linear from zero to 30 per cent on the temperature range, 60 degrees Centigrade to 100 degrees Centigrade.	

¹Properties shown are those perpendicular to the grain. See reference seven for detailed information on properties of balsa wood.

APPENDIX II

WIND TUNNEL TESTS TO CHECK VALIDITY OF EMPIRICAL FORMULAS
FOR EFFECTS OF TIP-PLATES AND OF THE PROXIMITY OF THE
GROUND ON WING INDUCED DRAG

Wind tunnel tests were conducted in the Georgia Tech 30 inch wind tunnel to determine the validity of the empirical formulas,

$$\frac{\Delta AR}{AR_g} = 1.9 \frac{z}{b}$$

$$\frac{\Delta AR}{AR_g} = 0.09 \frac{b}{h} ,$$

for the change in the effective aspect-ratio of a wing due to the addition of plates on the wing tips and due to flying close to the ground.

Four differently shaped tip-plates were used to determine the relative effect of the shape of the tip-plate on the effective aspect-ratio of the wing. In reference 2 it is stated that the height of the tip-plate was the primary variable in the effect of the tip-plate on the effective aspect-ratio.

The model used in the wind tunnel was an 0018 NACA airfoil constant chord wing with four differently shaped tip-plates (round, tear drop with point trailing, oval, and a very thin elliptical shape, i.e. the major axis was along the chord line and extending $0.3c$ behind the chord). Also, a ground plane (which could be adjusted to different heights below the airfoil varying from four chord lengths below the air-

foil up to the airfoil) was used.

The effective test R_n was 182,000. Test runs were made for both the wing alone configuration and for the wing with each type tip-plate. Then the ground plane was added, and the above configurations were repeated for several heights of the ground plane below the airfoil.

The height of the airfoil above the ground plane was measured from the top of the boundary layer to the 50 per cent station on the airfoil chord.

Within the scope of the test it was verified that the shape of the tip-plate did not influence the change in effective aspect-ratio of the wing. However, the profile drag, based on wing area, was increased due to the additional surface area added by the tip-plate.

The empirical tip-plate formula does not take into account the wetted area added to the wing configuration; consequently, the formula applies only for the change in effective aspect-ratio, i.e. the change in induced drag and the induced angle of attack.

Thus, at the low lift coefficients the increase in profile drag is greater than the reduction in induced drag gained by the tip-plates. Near a lift coefficient of 0.5 the two above conditions become equal, and above $C_L = 0.65$ it can be expected that the use of tip plates will result in a reduction of drag.

The results for these four configurations are plotted in Figure 2, and the values from the figure show that for the higher values of lift coefficient (at the low R_n) the empirical formulas were conservative.

Figure 2 shows an apparent reduction in drag on the wing at zero

angle of attack due to the presence of the ground plane in the wind tunnel. With the addition of the ground plane into the flow, re-attachment of the flow to the lower surface was accomplished at the lower angles of attack (see Figure 3). However, the re-attachment was complete on the wing without ground plane configurations above $C_L = 0.5$, and the results, thus obtained, are applicable and valid.

It is observed that for the wing configuration both with and without tip-plates there is an apparent low-drag bucket on the NACA 0018 wing. This was evidently due to flow separation over both top and bottom surfaces of the wing at the lower angle of attack, where the separation point moved rearward on the lower surfaces at a faster rate (with increasing angle of attack on the wing) than the separation point on the upper surface moved forward. Thus, the pressure drag was reduced with increasing angle of attack which caused the appearance of a low-drag bucket in the drag polar.

Therefore, it is seen that the empirical formulas for tip-plates and ground-effect are valid at Reynolds numbers at least as low as 182,000.

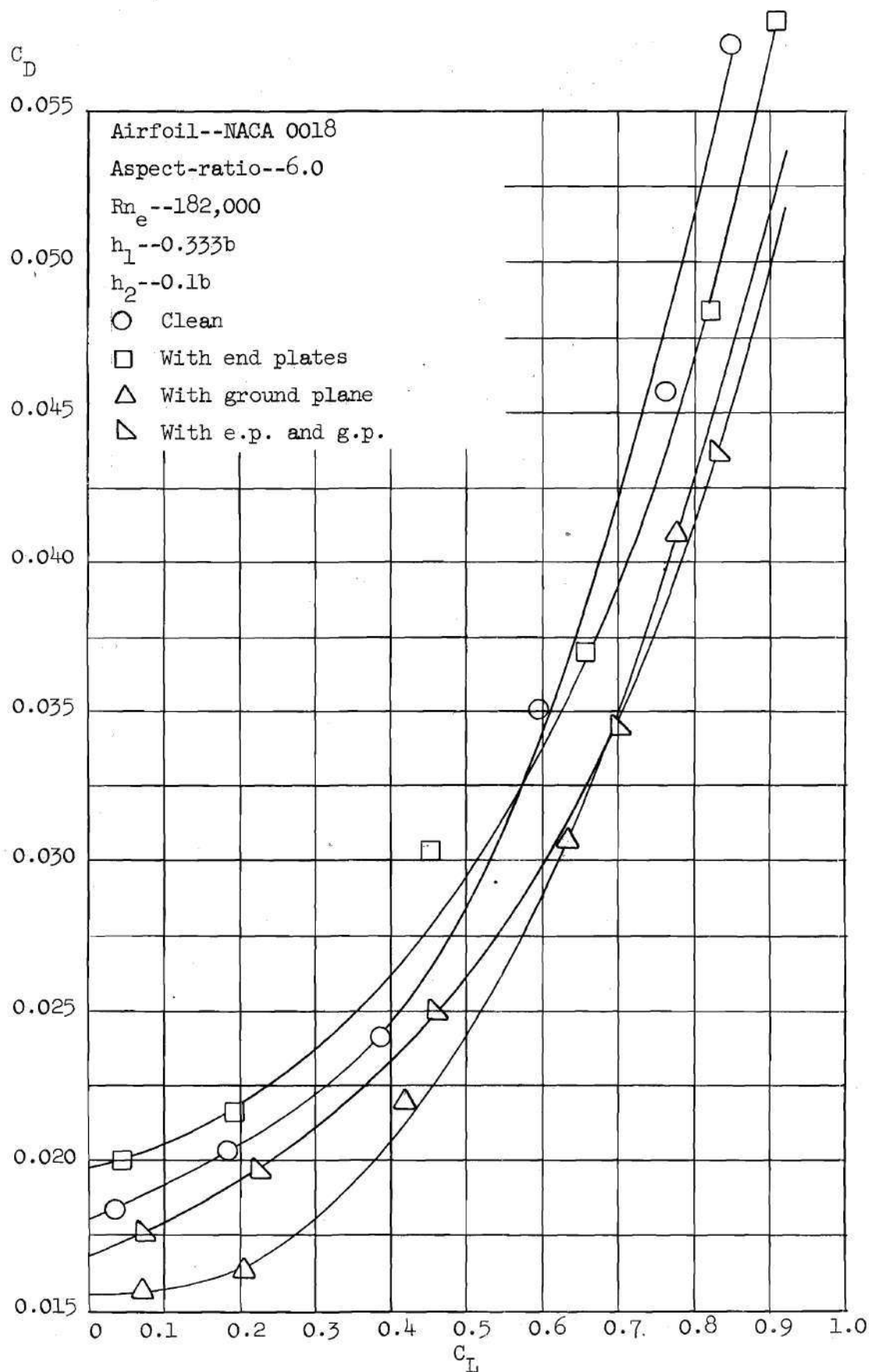


Fig. 2 Drag Polars for Four Configurations Tested

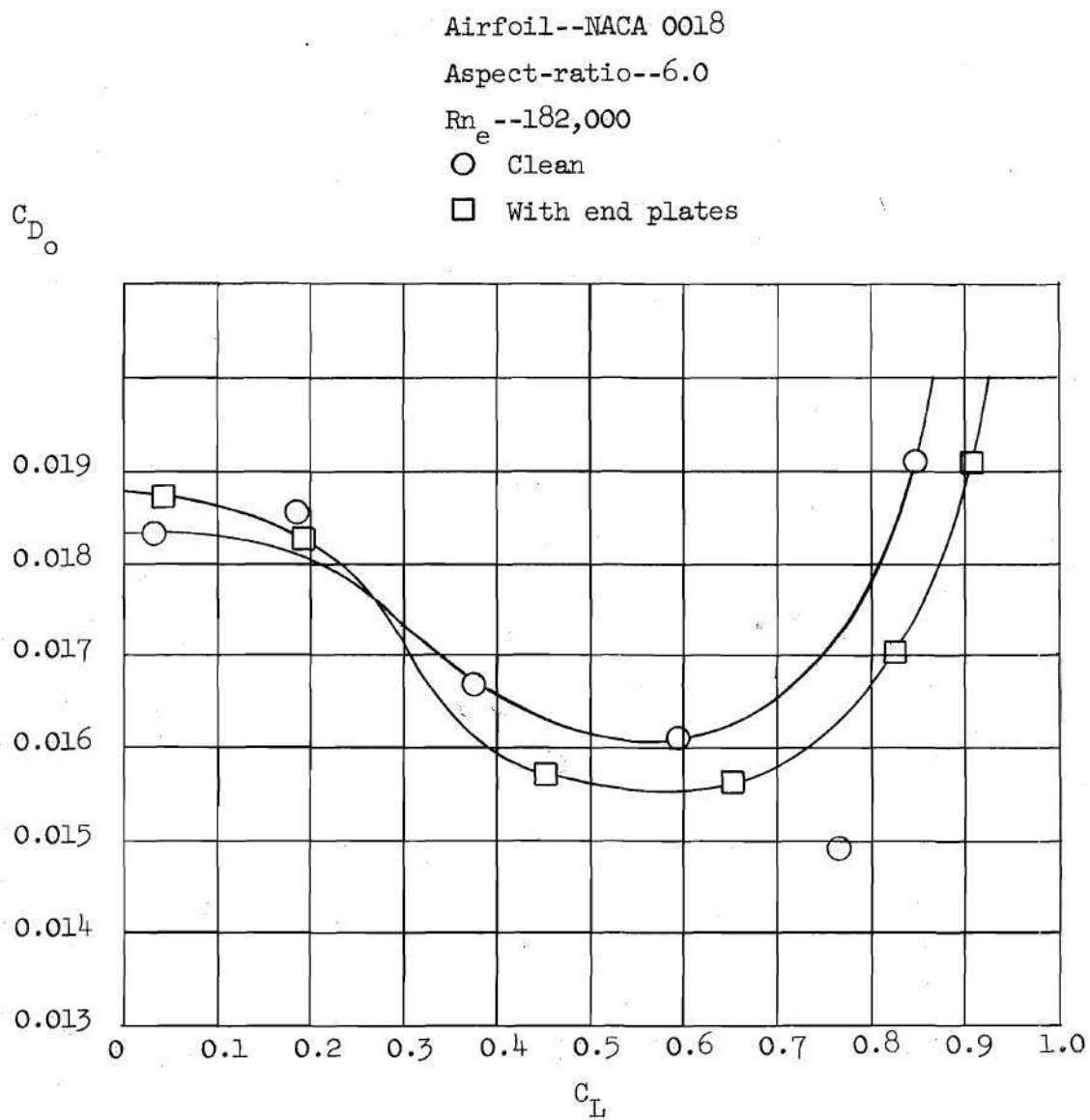


Fig. 3 Profile Drag Polar for Constant Chord Wing
Operating Out of Ground Effect

APPENDIX III

AIRCRAFT COMPONENTS AND WEIGHT ESTIMATION

Wing

The wing has a span of 54 feet, an area of 287 square feet, and is tapered 2.5 to 1. It has two truss type aluminum spars (see Figure 4) with balsa wood rib sections spaced every 12 inches. Figure 5 shows a typical rib section and the wing spars. Figure 6 shows the spars and ribs joined together. Figure 7 shows a completed semi-span including Mylar covering and the tip plate.

Wing Data

Area	287 sq. ft.
Span	54 ft.
m.a.c.	5.82 ft.
Taper	2 1/2:1
Front spar location	0.35 c
Rear spar location	0.60 c
C _{root}	7.60 ft.
C _{tip}	3.04 ft.
Airfoil	65 ₂ - 915 (NACA)
Rn of m.a.c.	1,310,000
Height of tip plate	30 inches
Length of tip plate	1.30 C _t

Chord length

7.6 - 0.169y ft.

Weight Estimation of Wing

Component	Number	Average Volume cu. ft.	Density lbs./cu.ft.	Weight lbs.
Spar caps	8	0.0103	175	14.5
Ribs	54	0.0161	10	8.7
Spar truss	8	0.0044	175	6.1
Glue	--	-----	---	2.0
Mylar	--	-----	---	3.2
Trail. edge	1	0.0105	175	1.8
Lead. edge	1	0.0390	175	6.8
Aileron Build-up	2	-----	---	1.5
Tip plate	2	-----	---	2.0
Root Build-up	8	-----	---	4.0
Total				50.6

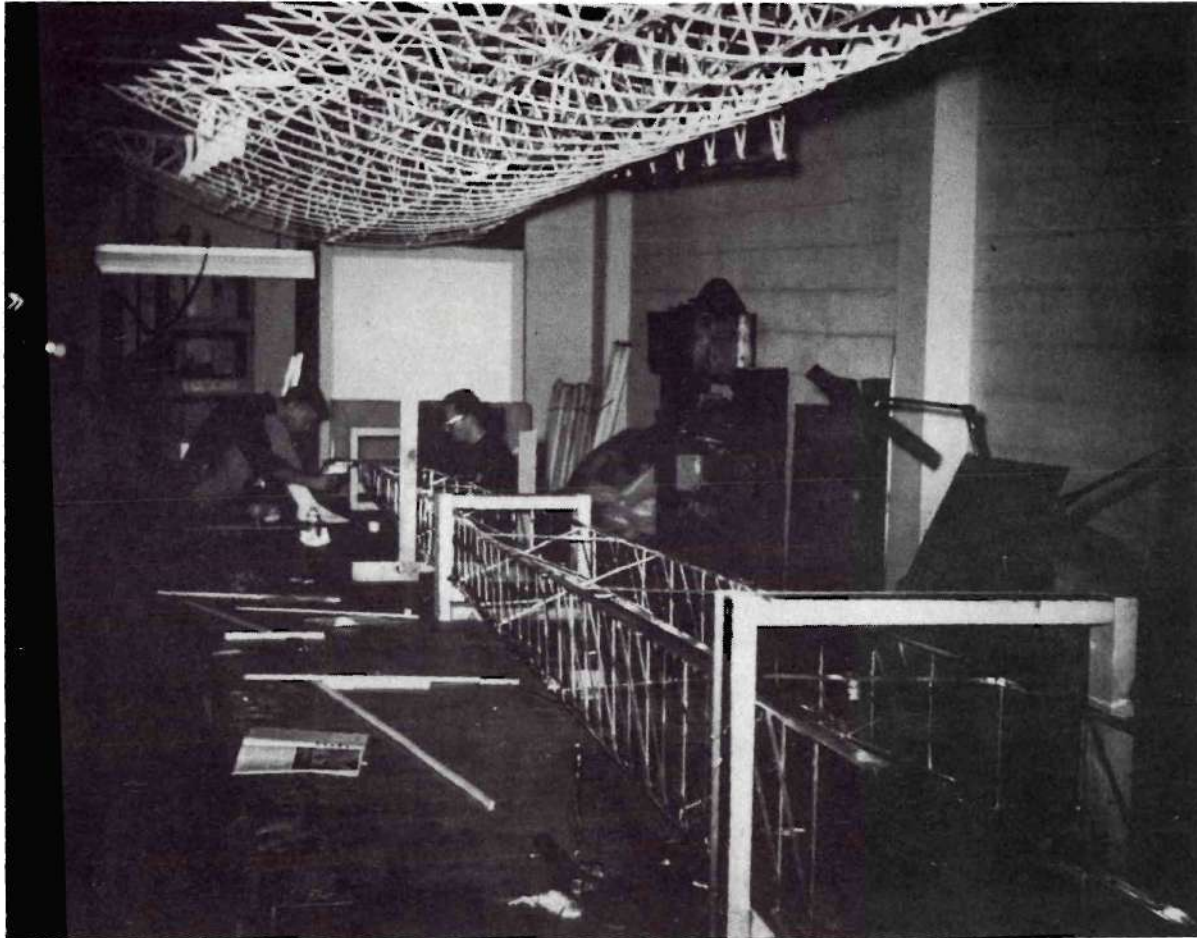


Fig. 4 Wing Spars

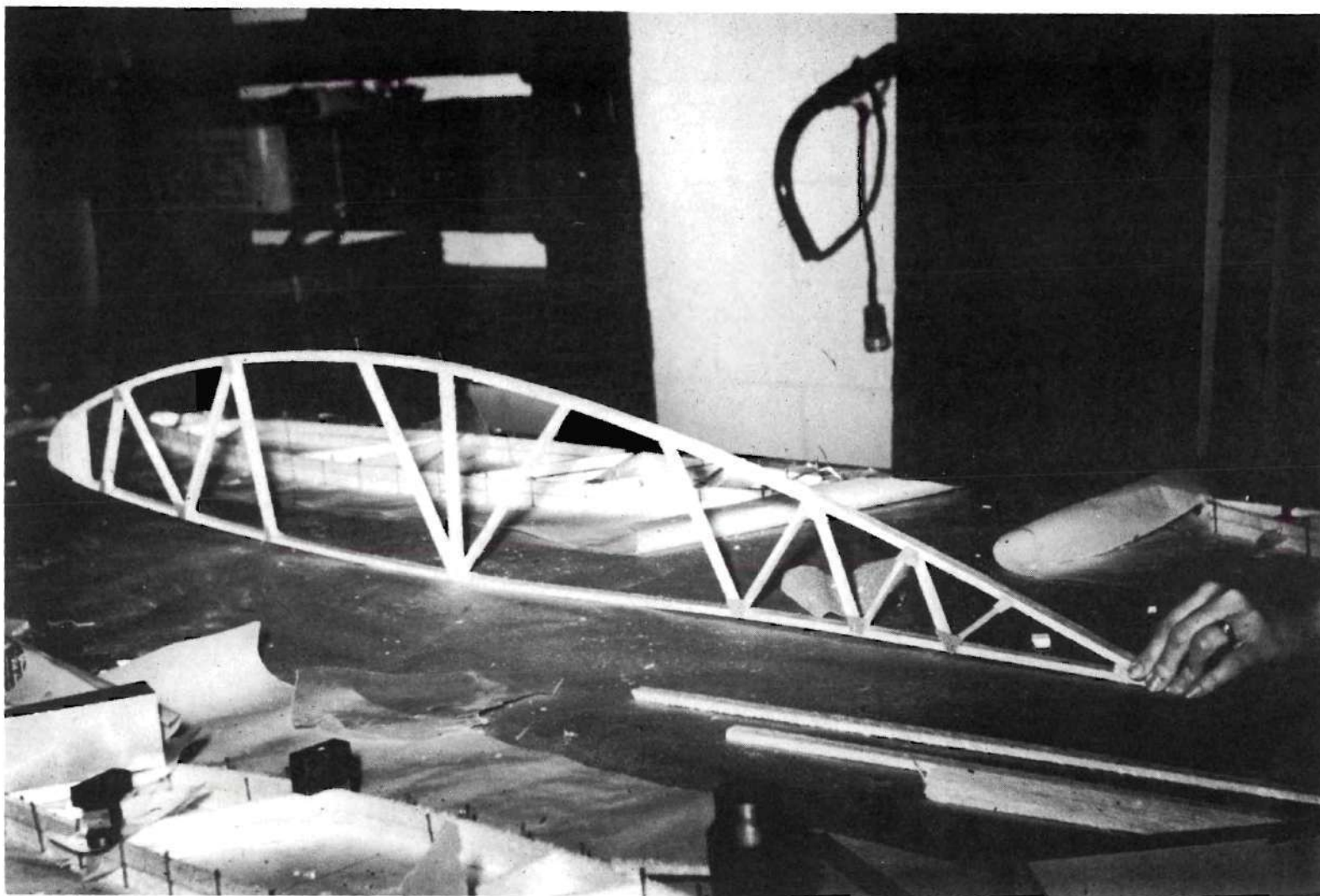


Fig. 5 Balsa Wood Rib Section

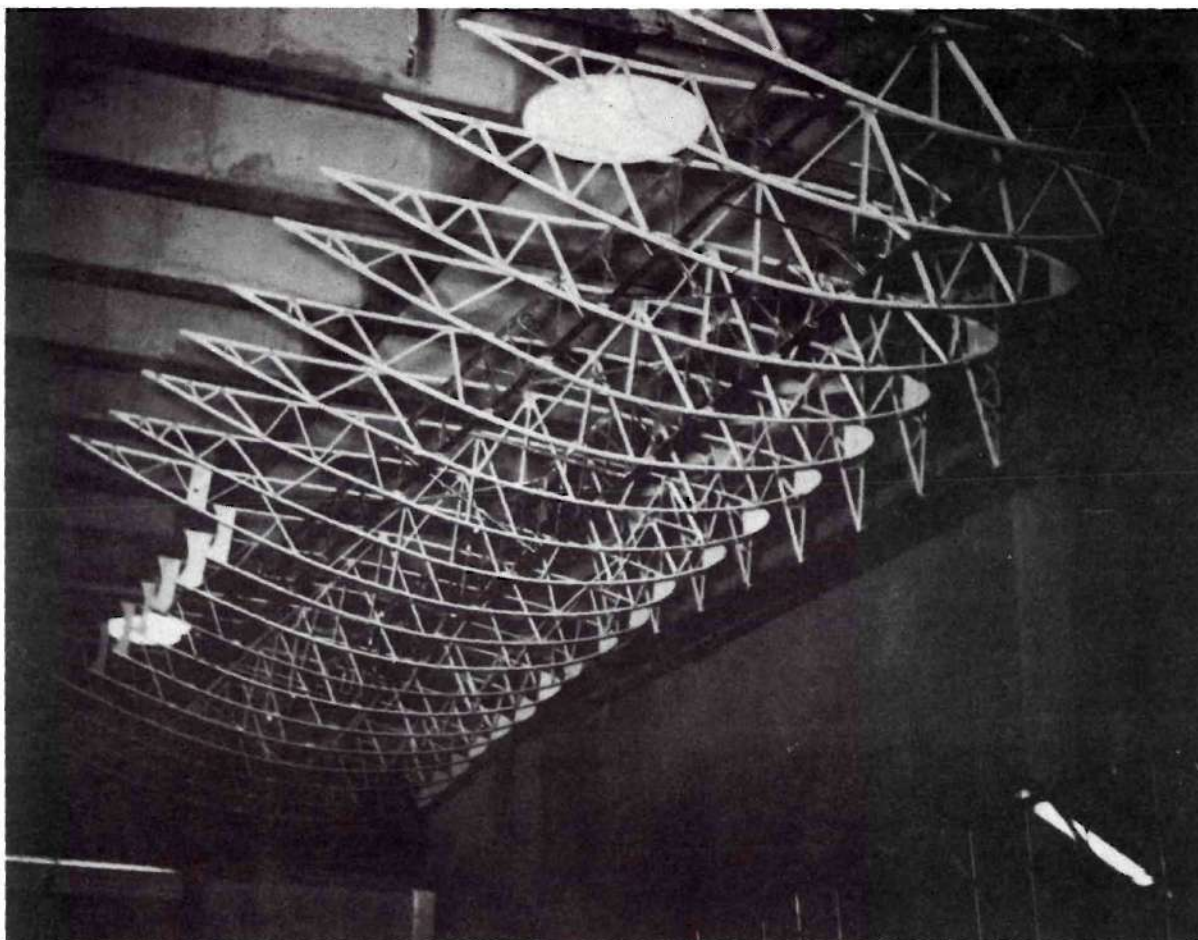


Fig. 6 Ribs and Spars Joined Together

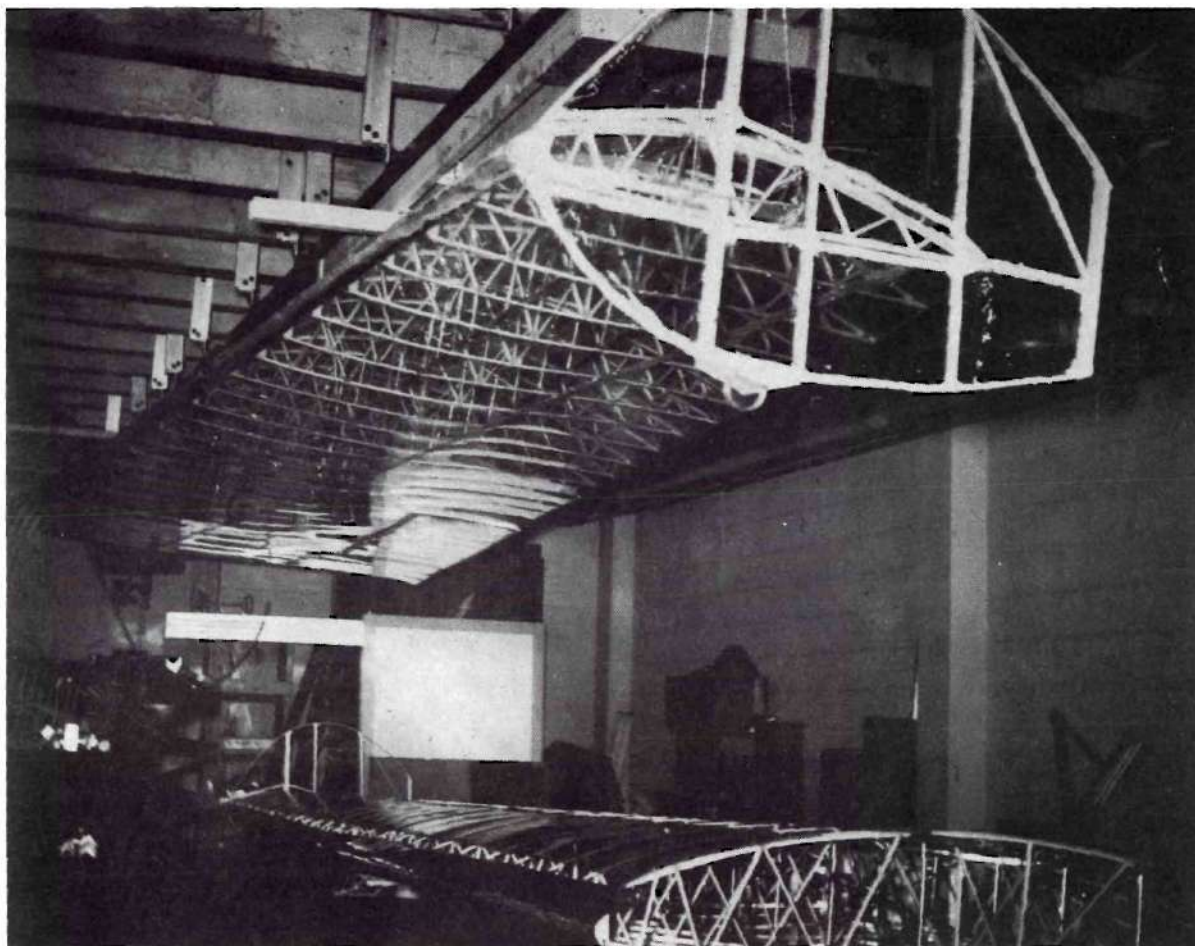


Fig. 7a Completed Wings Before Assembly
to Aircraft

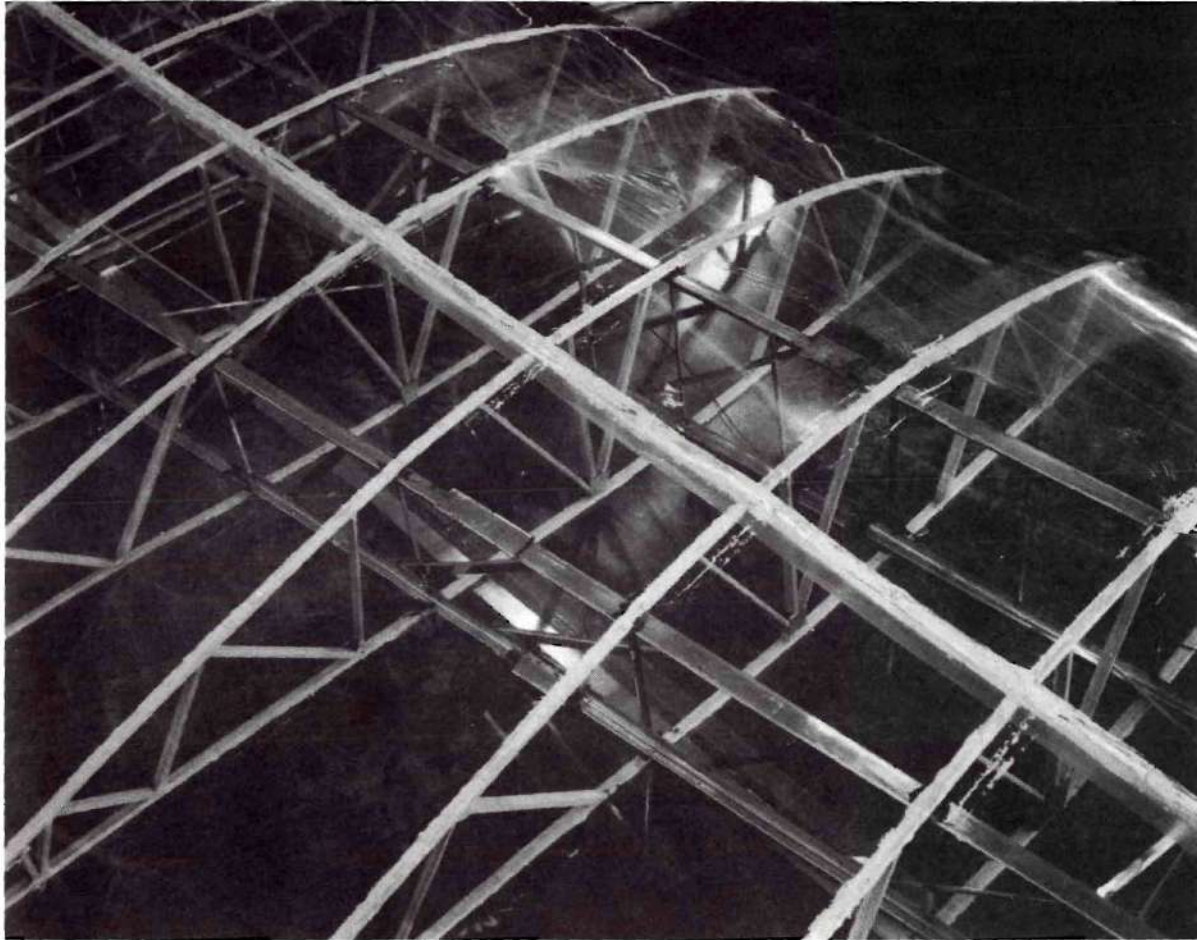


Fig. 7b Wing Internal Structure

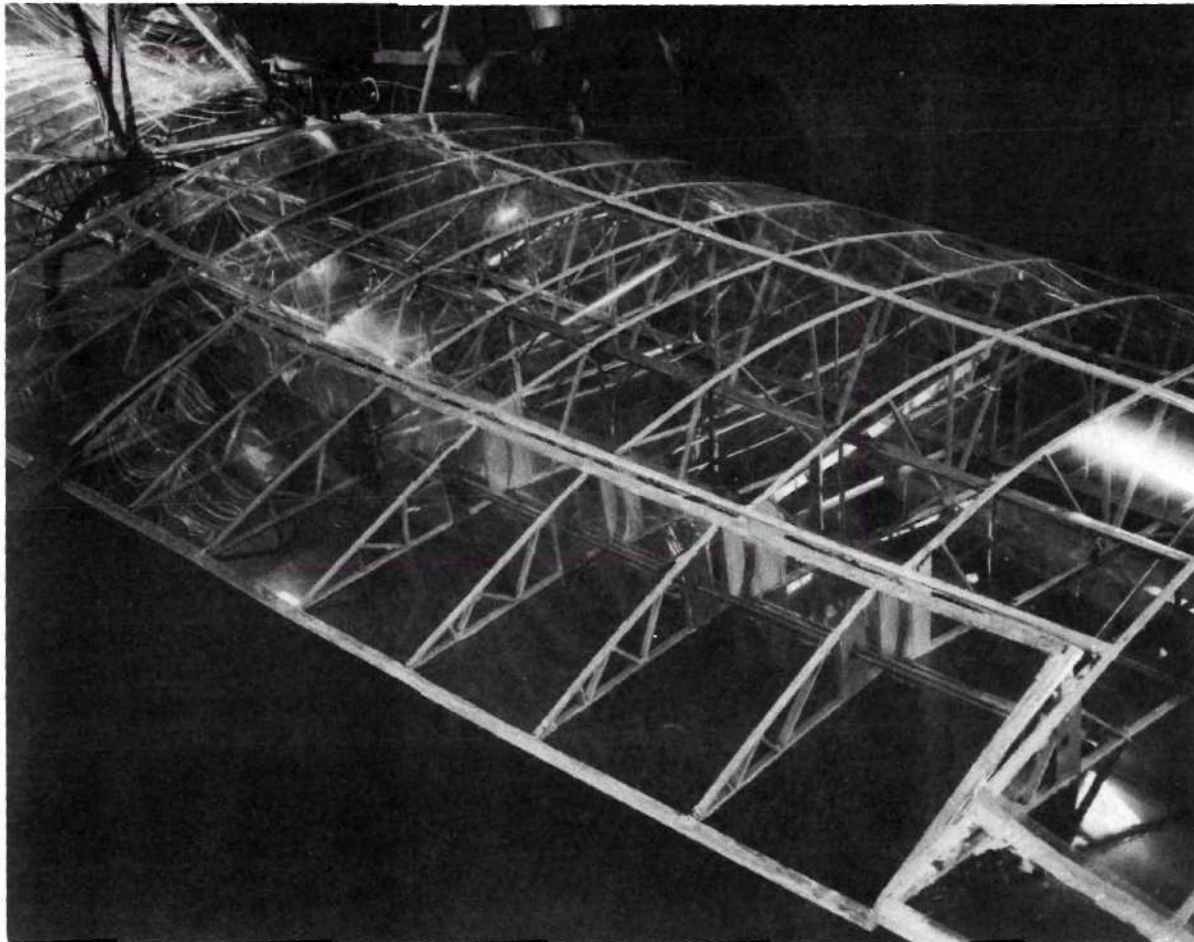


Fig. 7c Wing Section Showing Aileron

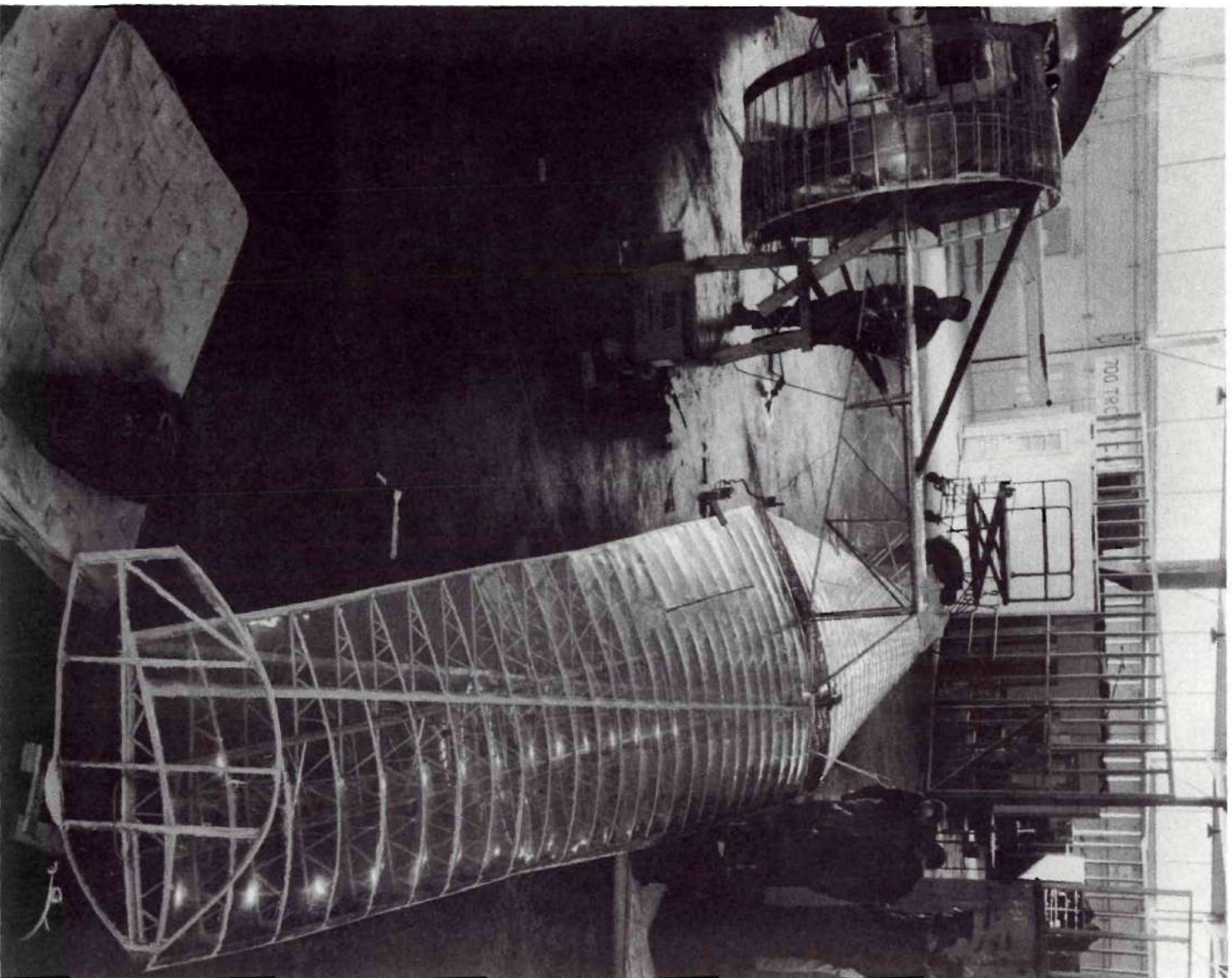


Fig. 7a Airplane Left Side View During
Final Assembly

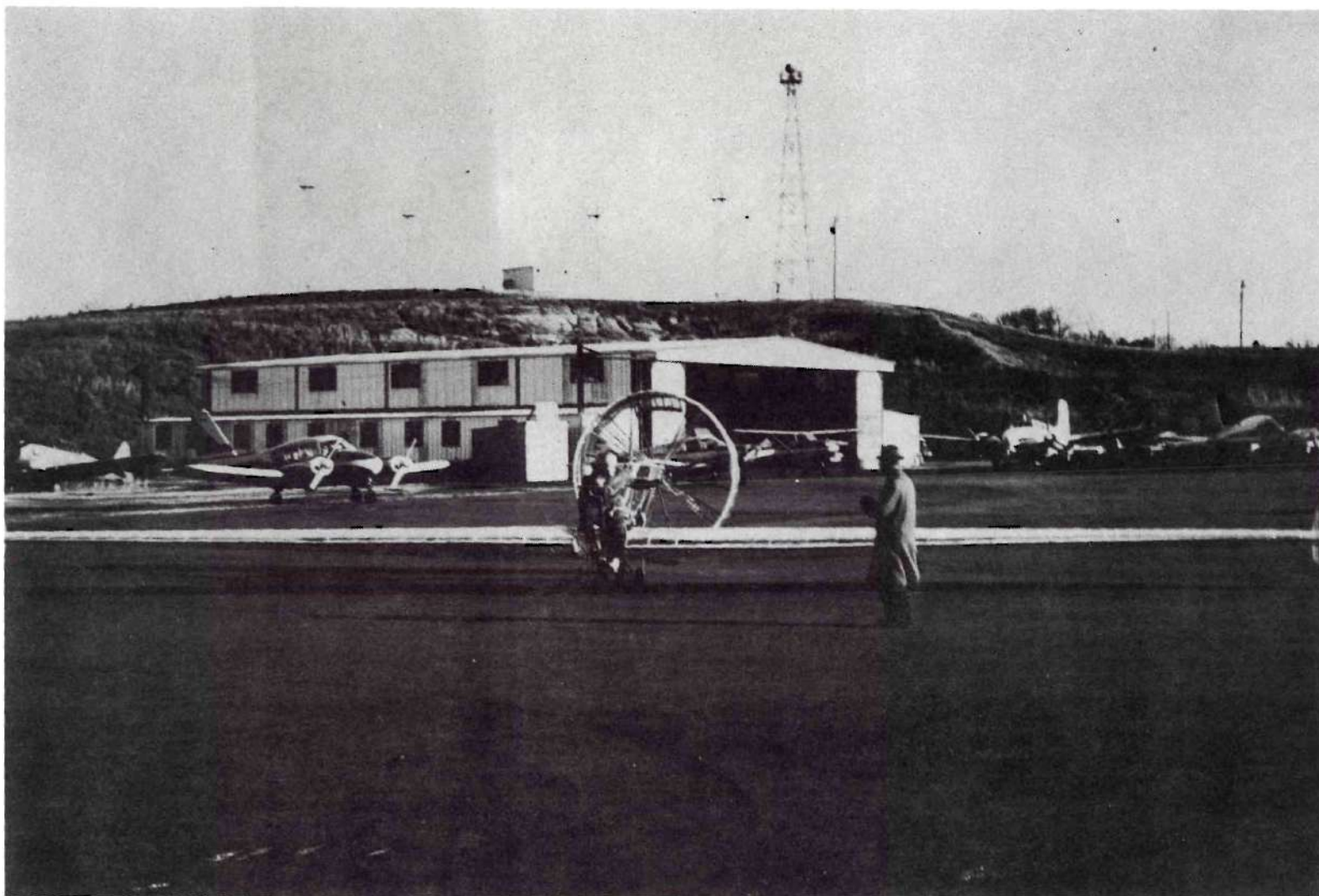


Fig. 7e Airplane Front View After Final
Assembly

The wing was weighed after this estimation was made, but before the Mylar was applied, and found to weigh 46.5 pounds. The Mylar weighed 3.2 pounds, giving a total weight of 49.7 pounds which is slightly under the estimated weight for the wings.

Fuselage

The weight estimates for the fuselage (see Figure 8 for the fuselage configuration) and propulsion system (see Figure 9 for propellers and shroud) were based on the amount of material needed, as was the wing weight estimate. However, it was more difficult to compute the exact weight of all members in the fuselage since the final configuration must be found and the airplane must be balanced simultaneously to insure that the center of gravity is located properly. Sixteen pounds were allowed for the shroud and propellers. This estimate is very accurate. Thirty-four pounds were allowed for the fuselage. However, it was found in the actual construction that the fuselage ran about 20 pounds overweight. This was caused primarily due to changes in the design of the fuselage during construction in order to take advantage of easier construction techniques and to speed up the building of the airplane.

Resultant Weight

Thus, the total weight of the entire airplane is 120 pounds--20 pounds over the estimated weight.

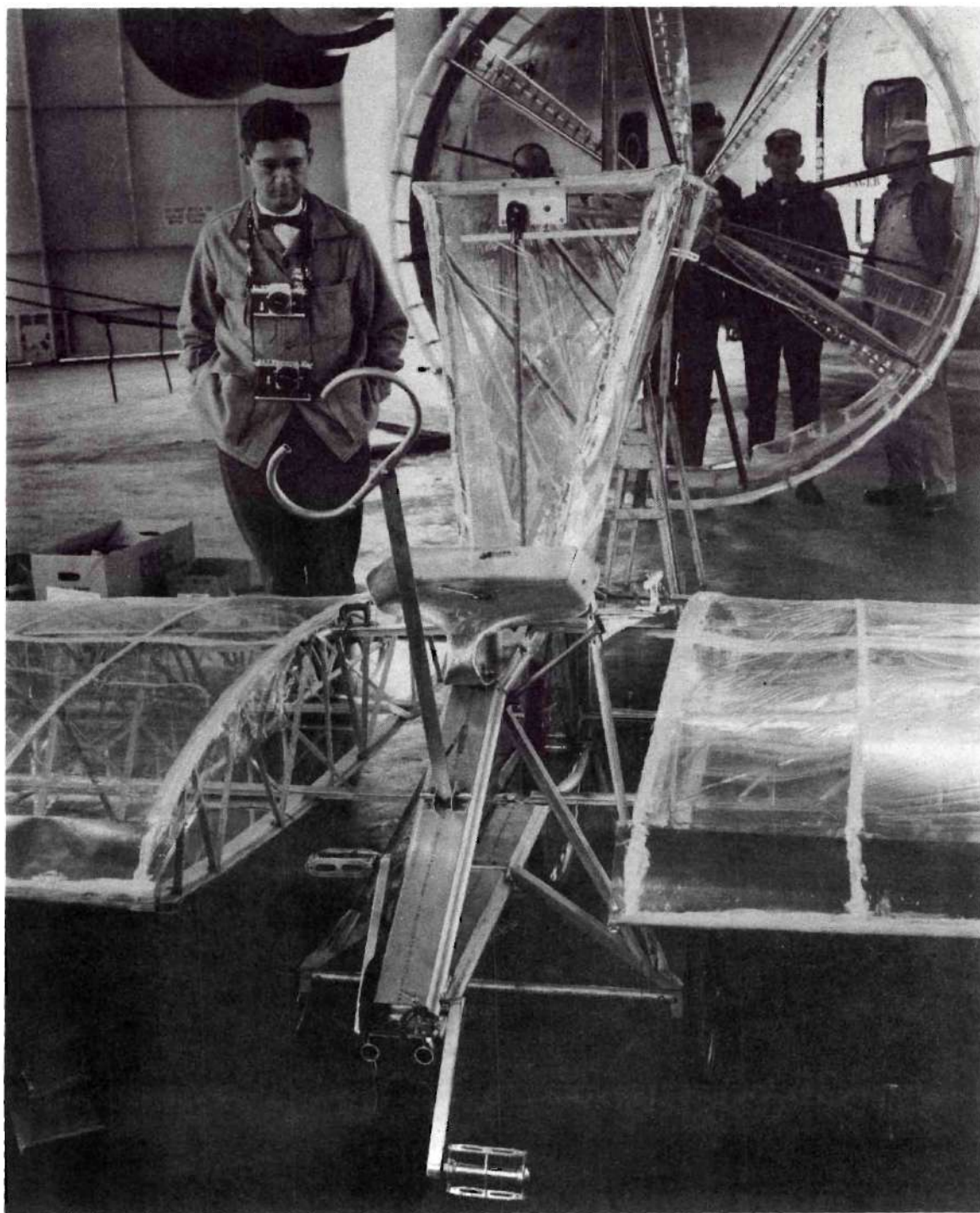


Fig. 8a Fuselage Front View

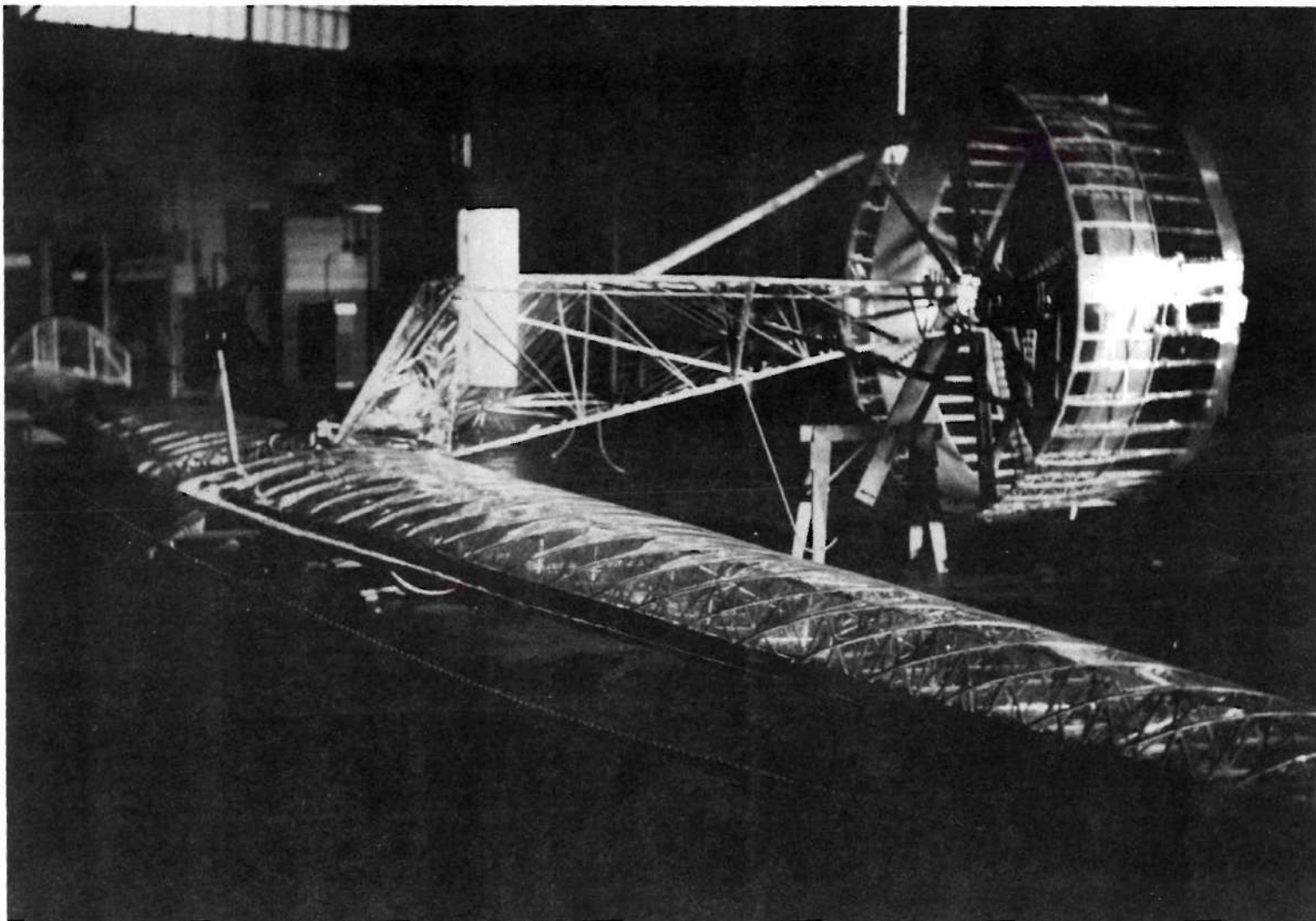


Fig. 8b Side View of Fuselage and Shroud

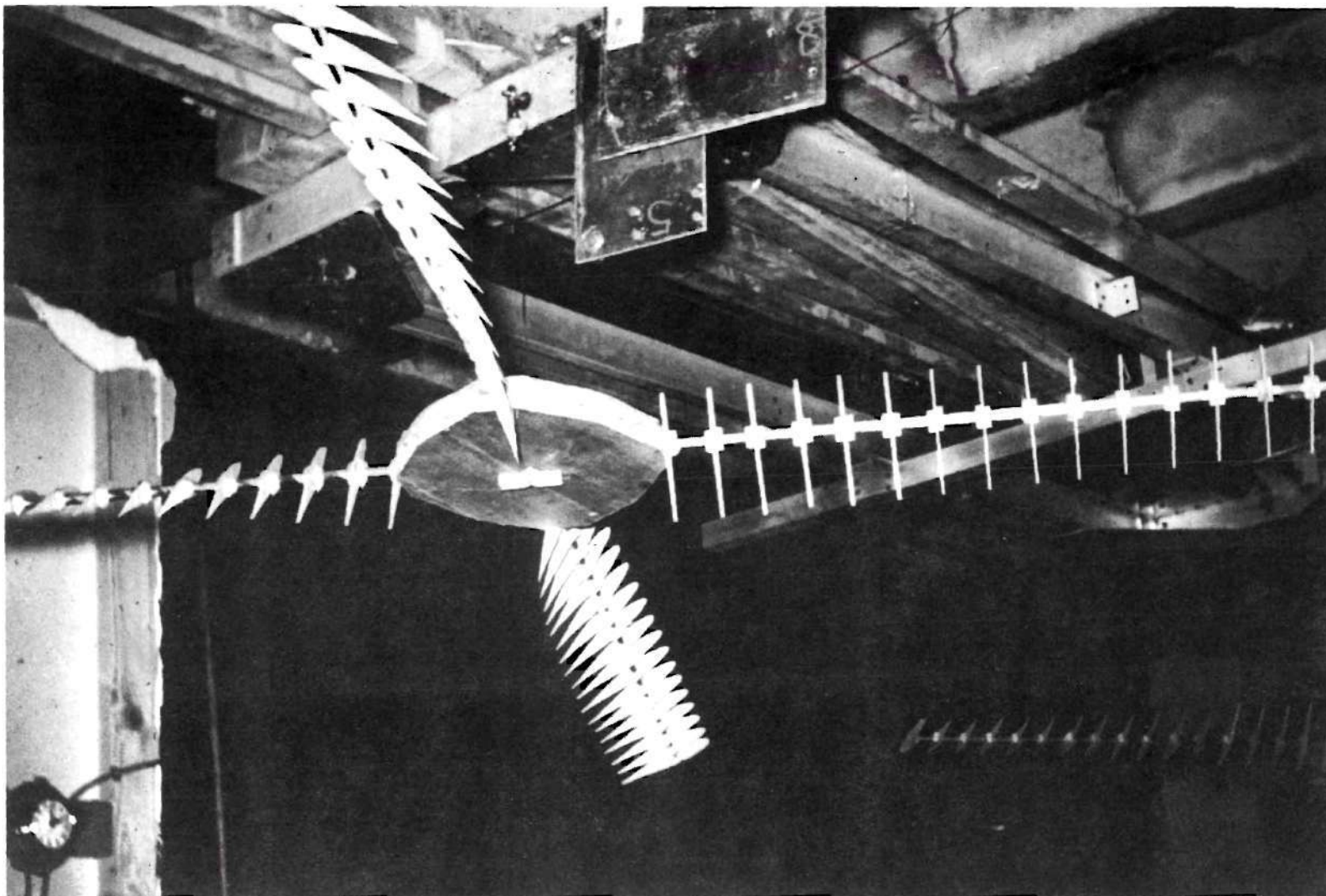


Fig. 9a Front Propeller During Construction

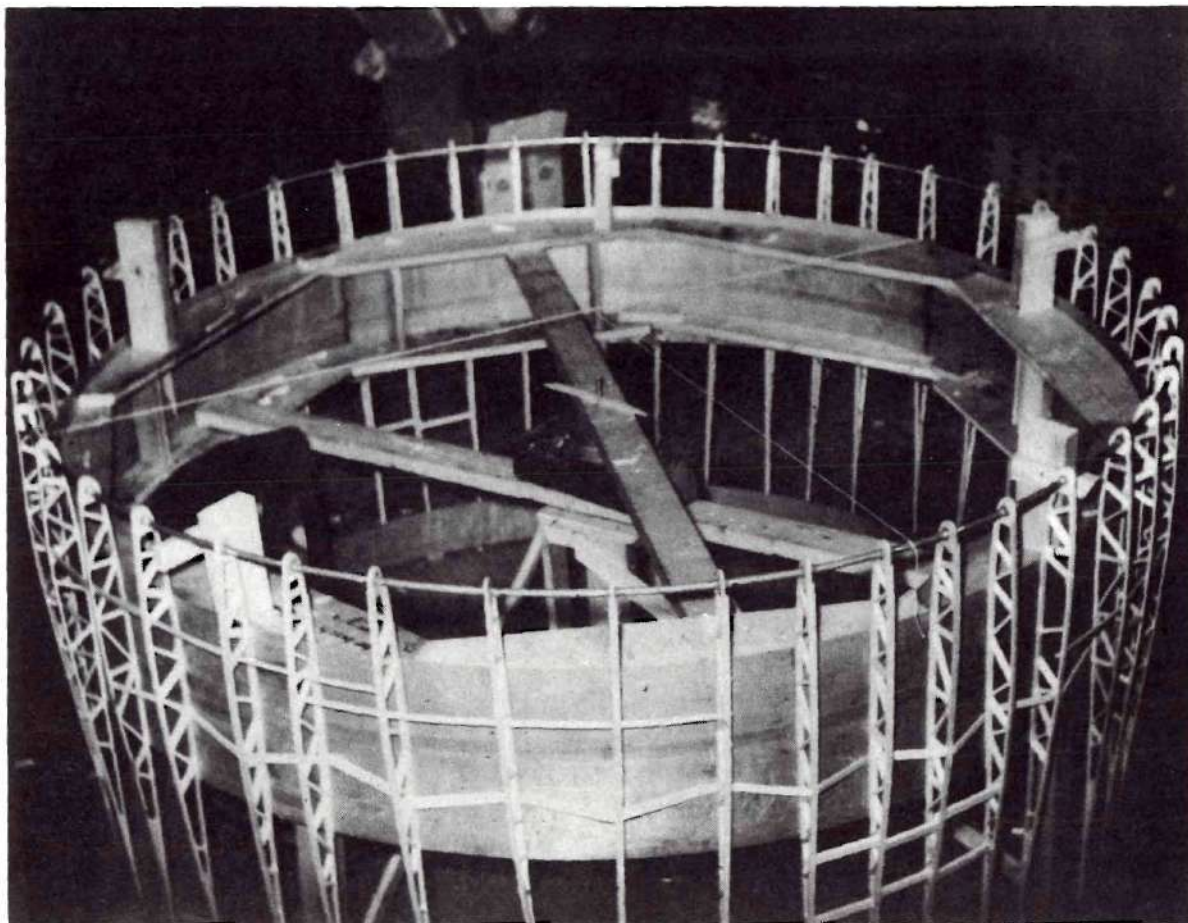


Fig. 9b Top View of Shroud While Jigged
During Construction

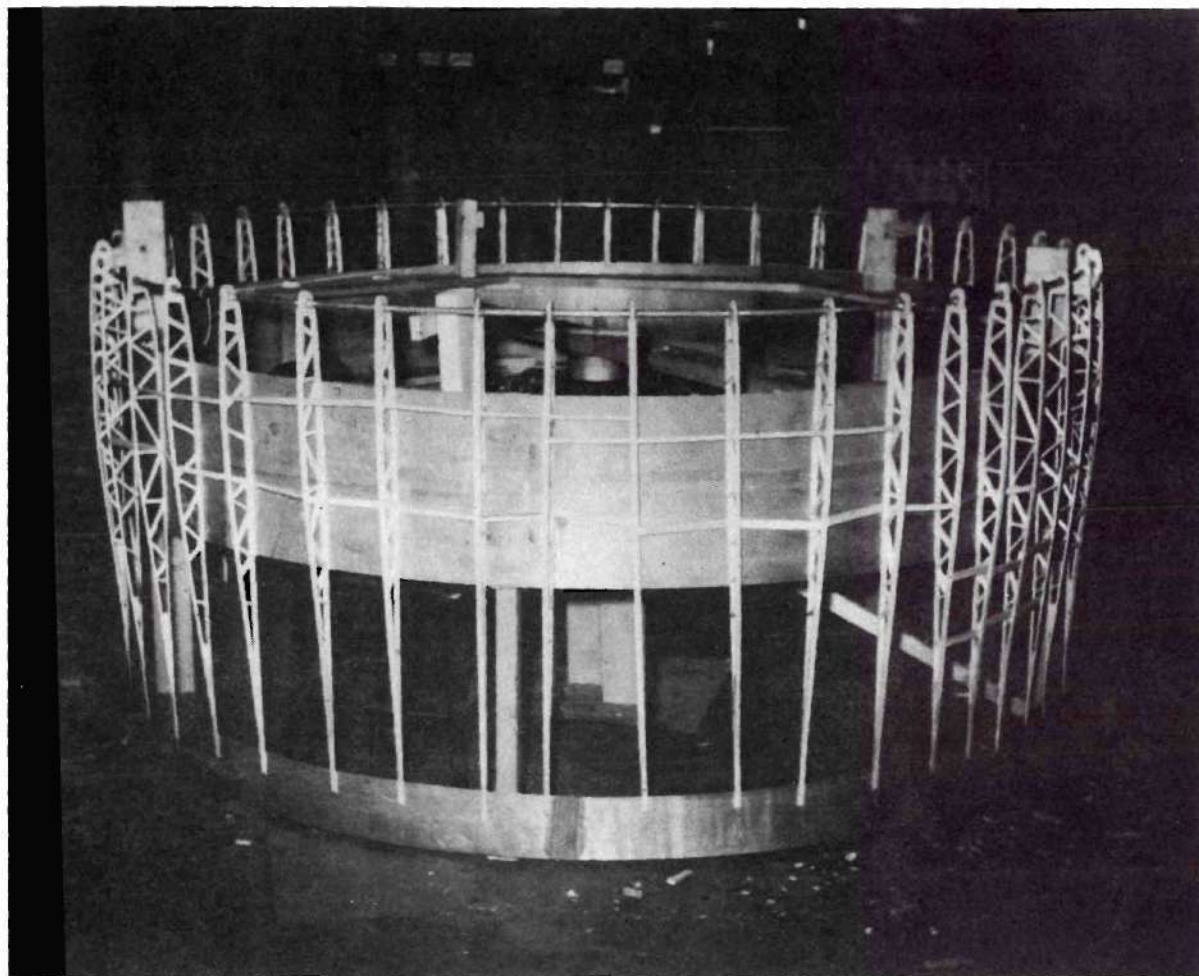


Fig. 9c Side View of Shroud During Construction

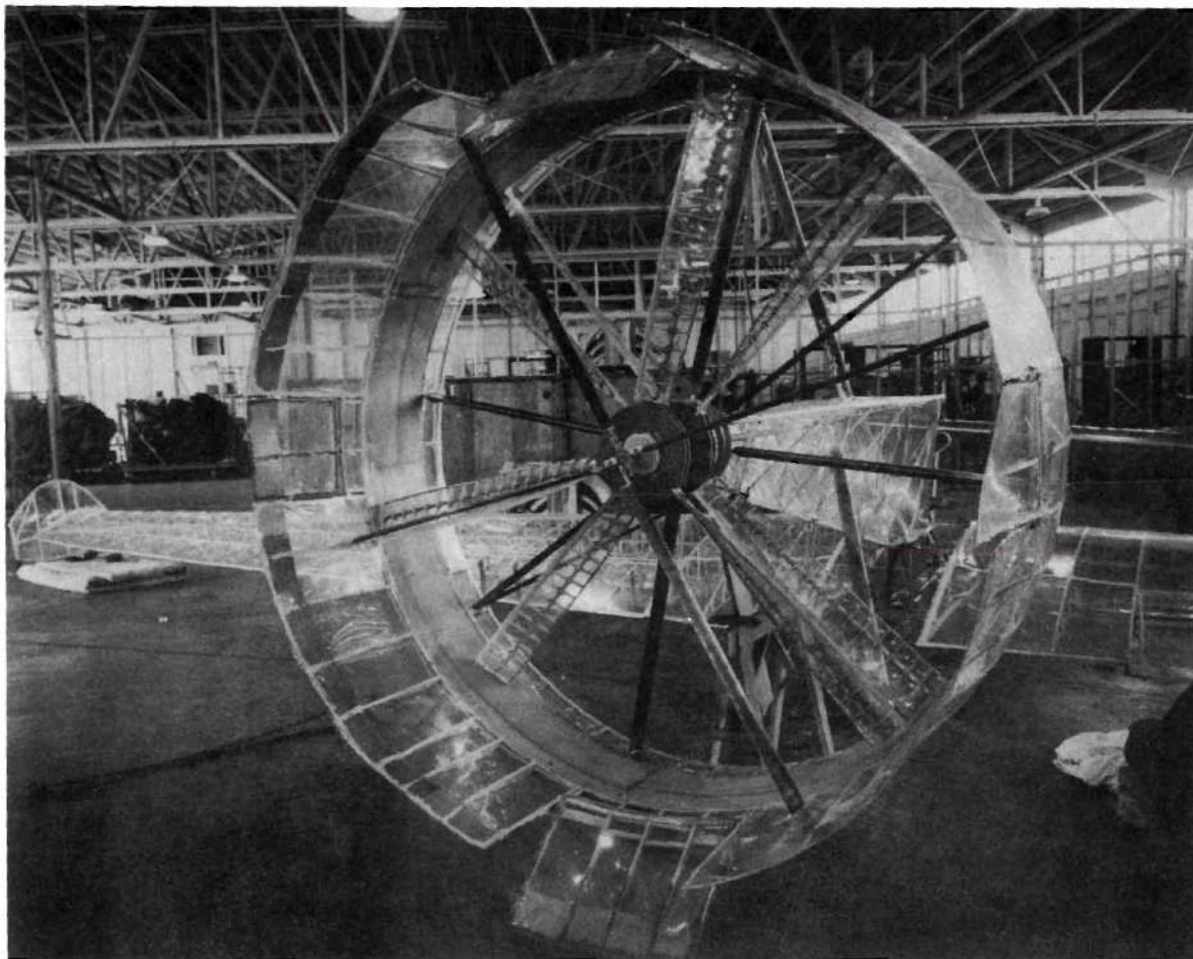


Fig. 9d Rear View of Shroud and Propellers
After Assembly to Aircraft

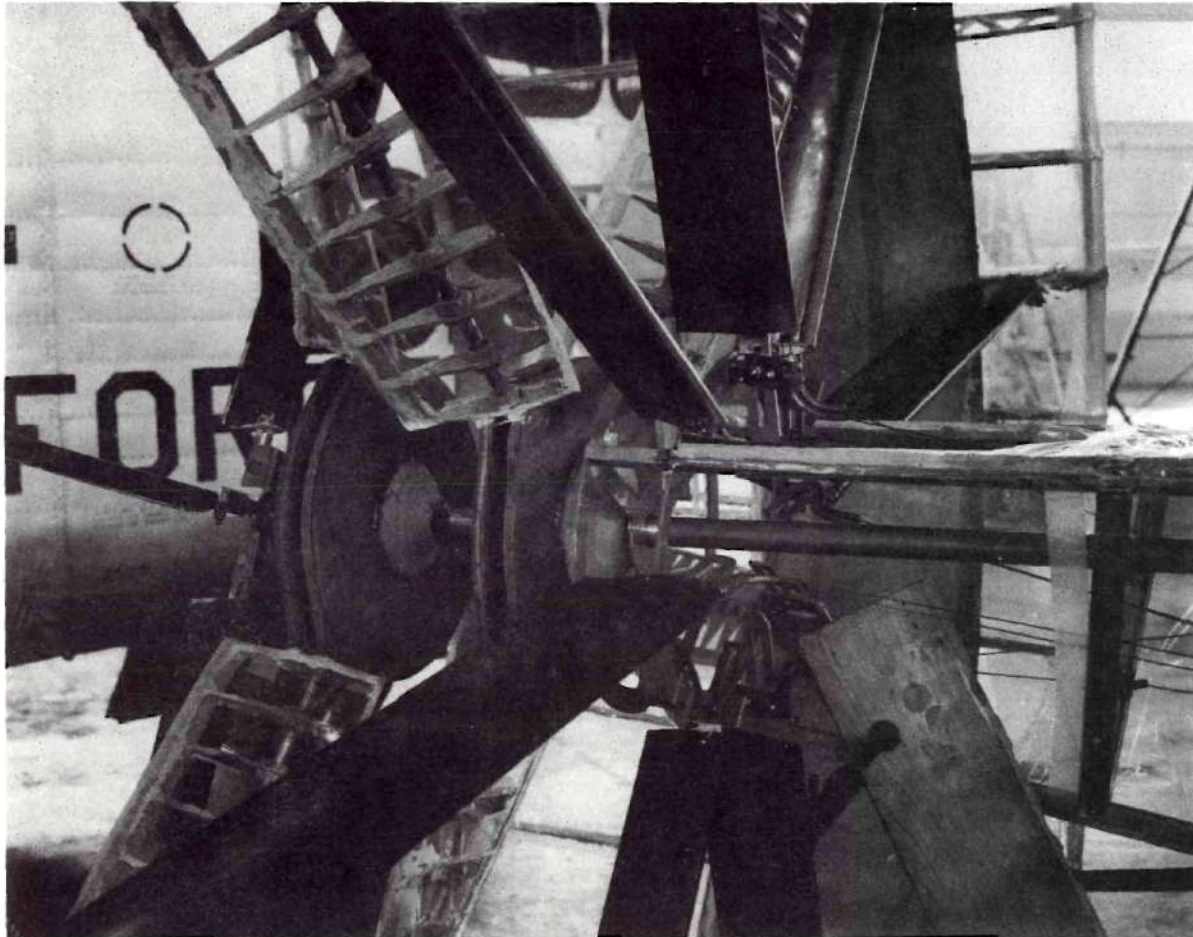


Fig. 9e Propeller Hub and Front Shroud
Mounting Struts

APPENDIX IV

WING PLANFORM SHAPE AND AIRFOIL SELECTION

It is very difficult to find the optimum wing configuration for any airplane, and it is even more difficult to find the optimum wing configuration for a human-powered airplane. This is because there are four primary variables to be considered: weight, drag, velocity, and structural strength. On most conventional designs, the weight and horsepower available are known. Thus, only drag and structural strength have to be considered.

It was observed that the airfoil profile drag is fixed for a given angle of attack and Reynolds number. Therefore, the induced drag is the primary drag variable. Different wing planform configurations were investigated to find one or more that would give good values for the primary variables (holding profile drag as a constant equal to zero). The NACA airfoil data was studied to find an airfoil that would give allowable profile drag characteristics under the conditions imposed by the wing configuration and power limitation.

In order to study the wing planform configurations, a computer program was used in which the lift coefficient was varied in increments of 0.1 from 0.6 to 1.5, the flight velocity was varied in increments of 2 feet per second from 26 feet per second to 40 feet per second, and the wing span was varied in increments of 2 feet from 40 feet to 60 feet.

The corresponding wing area and induced drag were computed for each combination of C_L , V , and b above. It was concluded that a

large value for the wing span coupled with a medium value for the lift coefficient would give a low value for the induced drag and an acceptable wing planform area; however, Reynolds number effects and structural strengths were yet to be considered (see Appendix V for wing stress analysis).

After studying the NACA airfoils it was concluded that a laminar-flow airfoil would be used which would give very low values for the profile drag for relatively large lift coefficients. Figure 10 shows that there is negligible change in the minimum profile drag of an airfoil section with change in lift coefficients up through $C_L = 1.78$ at a Reynolds number of three million. A similar result is found in reference 5 for a Reynolds number of six million.

Thus, it was determined (for a given laminar-flow airfoil family with constant thickness and at a constant Reynolds number), that the profile drag polar is very nearly of constant shape with the low drag bucket centered over the design lift coefficient.

The NACA 65₂-915 airfoil was selected for use on the human-powered airplane, and an excellent set of drag polars was found (see Figure 11) for Reynolds numbers ranging from 230,000 to 9,000,000.

The final wing configuration has a span of 54 feet, area of 287 square feet, and a 2 1/2 to 1 taper. The airfoil is an NACA 65₂-915 for all stations, and there was no twist in the wing. The Reynolds number based on the mean aerodynamic chord is slightly over one million.

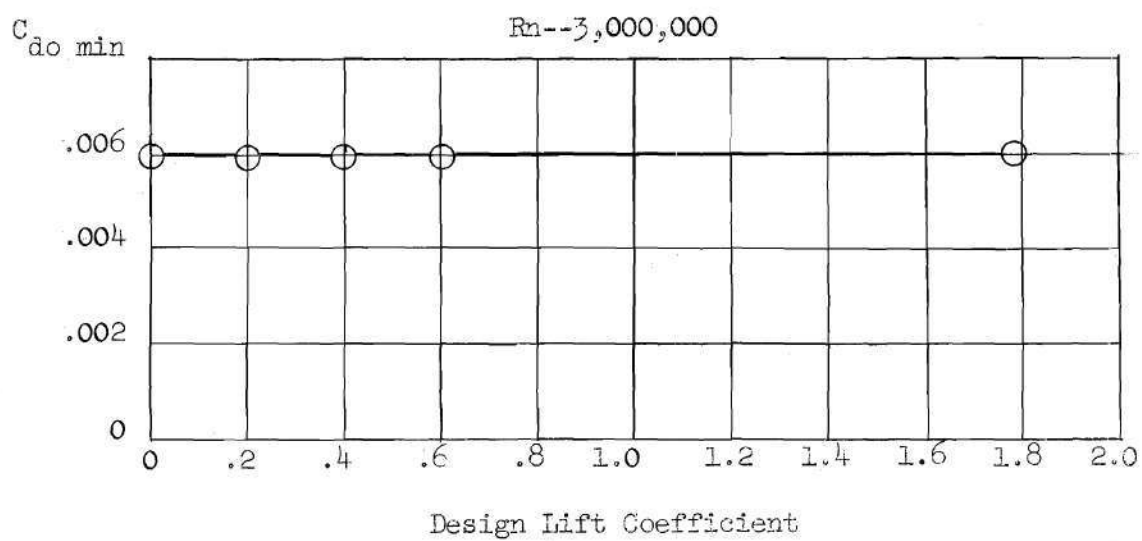


Fig. 10 Camber Effect on the Section Minimum Drag Coefficient of Thick NACA Laminar Flow Airfoils as Taken from the NACA Data

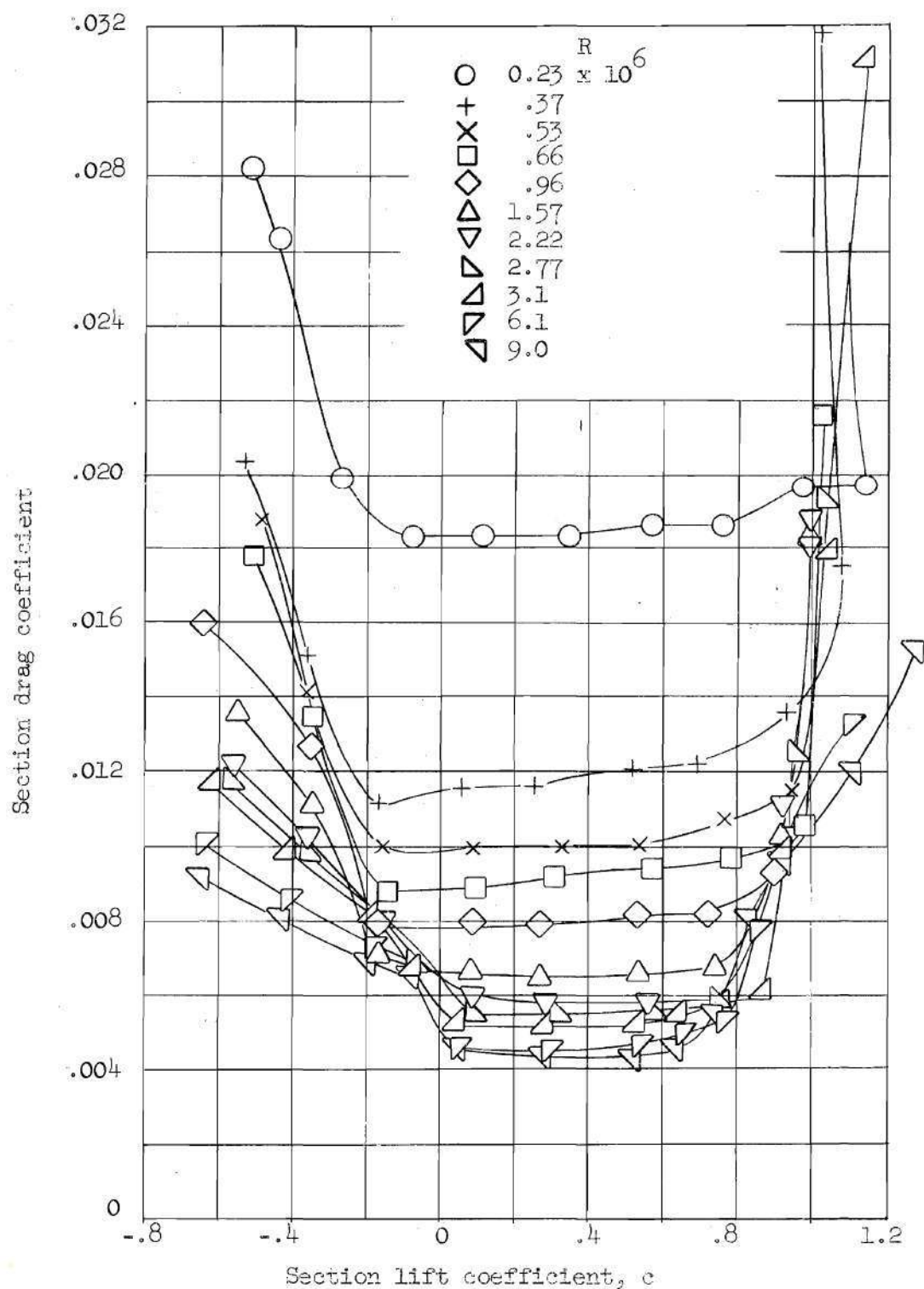


Fig. 11 Section Drag Characteristics of the NASA 65,418 Airfoil
Taken from the War Time Report, ACR Number 74H11

APPENDIX V

WING STRESS ANALYSIS

The wing structure must be strong enough to support 1.125 times the gross weight of the airplane. In order to simplify the computations, it is assumed that all of the load is carried by the wing spar caps. This is somewhat conservative, since the lower skin will take tension while the leading and trailing edge of the wing will also take tension and compression as well as shear. In order to insure good controllability of the aircraft and to maintain desirable aerodynamic characteristics across the wing, it is imperative that the wing deformations be small. Thus, the deflections due to wing bending must be less than 10 per cent of the wing semi-span. Due to the difficulty in computing the torsional rigidity of the wing, diagonal tension strips were added on both the upper and lower surfaces to give increased resistance to torsion, and to insure that the wing does not twist excessively.

The wing loading is considered to be constant over the wing-span, adding to the conservative nature of the computations. The two spars in the wings are of the truss type with spar caps for the main members. It is assumed that the spar caps take all the loads, with the truss members restraining the spar caps under compression from buckling.

The buckling loads are computed by the Euler formula with the effective lengths assumed to be eight inches (two-thirds of the distance between ribs). However, the maximum truss member spacing is four inches apart along the spar cap.

The spar caps were formed by rolling a sheet of 0.02-inch thick 2024-ST aluminum into a "T" section, where the two edges of the sheet meet at the bottom of the "T". The width of the sheet used in each spar cap is given by the formula:

$$\text{width} = (4.13 - \frac{2.755}{27} y) \text{ inches} .$$

The chord length at any station is

$$C = (7.6 - 0.169 y) \text{ feet} .$$

The spars are located at the 35 per cent and 60 per cent chords, and the depths of the spars are the thickness of the wing at the spar cap minus 1/2 inch.

It was found that the maximum stress is at the root section.

The root bending is:

$$M = (162 \text{ lbs.})(13.5 \text{ ft.}) = 2190 \text{ foot pounds} .$$

The area of material resisting this moment is

$$A = (2)(4.13)(.02) = 0.165 \text{ square inches} .$$

The average depth of the root section spars is one foot. Thus, the resulting tensile stress is 13,300 pounds per square inch, and the average load resisted by each spar cap is 1095 pounds.

The Euler formula for buckling is

$$P_{cr} = \frac{2 EI}{L_e^2}$$

$$E = 10^7 \text{ psi}$$

$$L_e = 8 \text{ in.}$$

$$I = 0.000744 \text{ (in.)}^4$$

which gives

$$P_{cr} = 1140 \text{ pounds .}$$

The bending deflections of the wing tip is computed from the bending energy formula for deflection

$$\text{deflection} = \int_0^{b/2} \frac{Mm \, dy}{EI} .$$

The bending moment is

$$M = \frac{1.125}{54} W \frac{y^2}{2} .$$

The bending due to a virtual load of one pound applied vertically at the wing tip is

$$m = (1) y .$$

The moment of inertia of any section is

$$I = \left[(0.066)^2 \right] + (0.05)^2 \cdot (\text{chord})(2)(A_{\text{spar}}) .$$

$$\text{chord length} = (7.6 - 0.169y) \text{ 12 inches}$$

$$\text{area spar cap} = (0.02)(4.13 - 0.102y)(\text{in.})^2$$

The resulting tip deflection is 23.6 inches--7.4 per cent of the semi-span length.

The leading edge strip is not continuous across the center of the plane as the strip would interfere with the pedals. No provision was made prior to the first flight attempt to join the inboard end of the leading edge strip to the rest of the fuselage other than through the balsa wood ribs. The leading edge strip carried considerable bending and shear stress. Naturally, the stresses went to zero or to the small value that could be transmitted through the balsa wood rib at the discontinuity. Due to the discontinuity in the leading edge strip, the shear center of the wing also had a discontinuity in this region. Over the wing where the leading edge strip is in place, the shear center (experimentally determined) is aligned with the center of pressure within about one per cent of the chord for any wing section. However, at the inboard section the shear center is located very nearly at the center of gravity of the spar caps, which is well behind the center of pressure of the m.a.c.

The Euler buckling loads were computed assuming that the spar caps remained straight under loading. However, with the center of pressure considerably ahead of the shear center on the inboard wing section, the wing twisted over this area causing the spar caps to twist out of their initially straight condition. This allowed the spar cap under compression to deflect out of its normal plane. Since the true loads were very near the buckling load, the deflections became quite large. It is prob-

able that the flange on the spar cap "T" experienced local crippling under such a large deflection, thus lowering the Euler buckling load as there was less material acting effectively after the local crippling occurred. This conclusion is supported by observation of the nature of the failure. The buckling occurred out of the plane of the initially straight spar cap in the direction dictated by the twisting moment present on the wing. Further, the top of the ribs pulled loose from the front top spar cap starting with the inboard rib out to about the twelfth rib, as each succeeding rib tried to resist the twisting moment from the leading edge strip. By taking hold of the out-board section of the wing and applying a nose-up twisting moment, it could be seen that the resulting deflections of the broken ribs were in the direction taken at breakage. The nose-up twisting moment is in the same direction as the aerodynamic twisting moment on the wing.

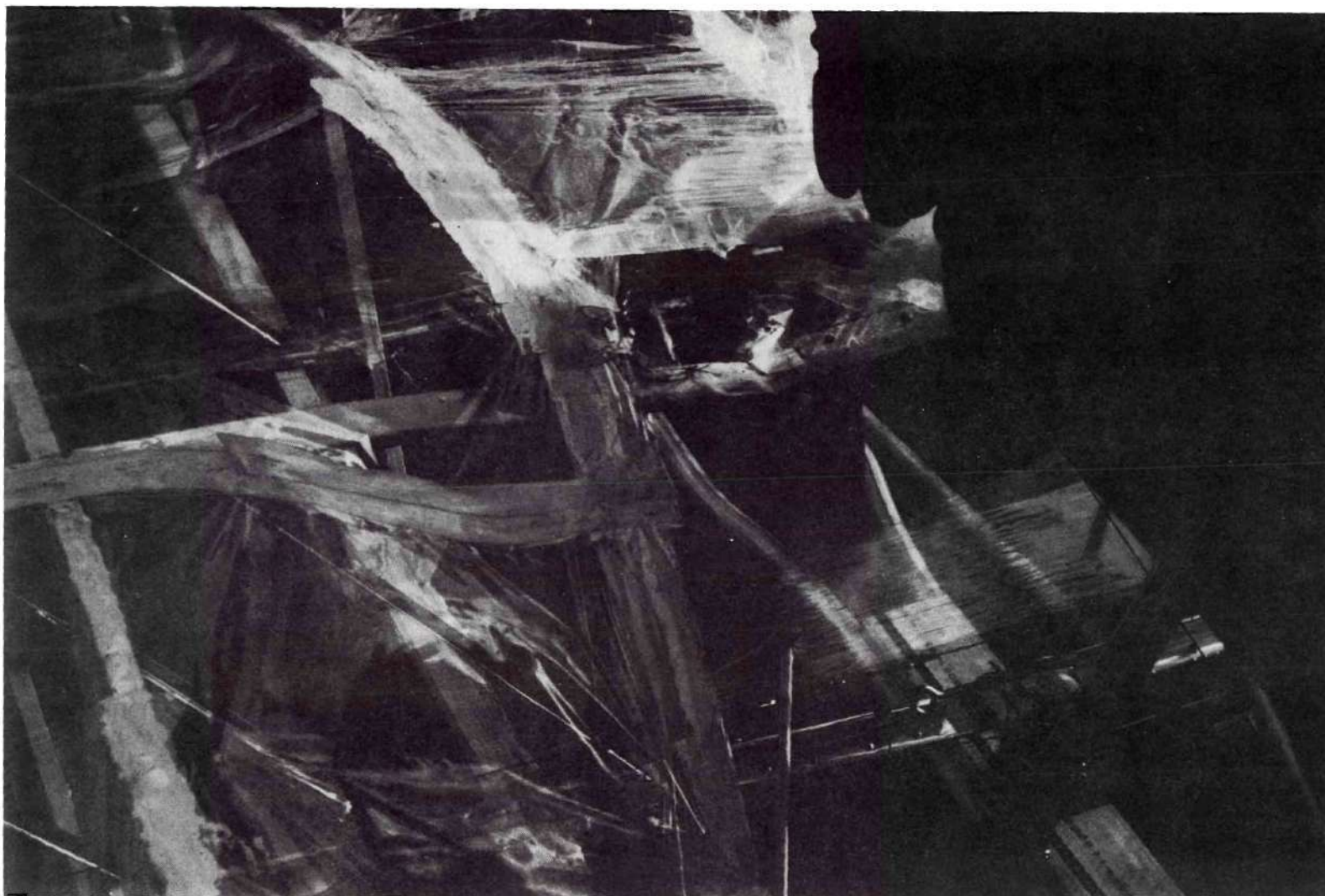


Fig. 12a Top View of Buckled Spar Cap

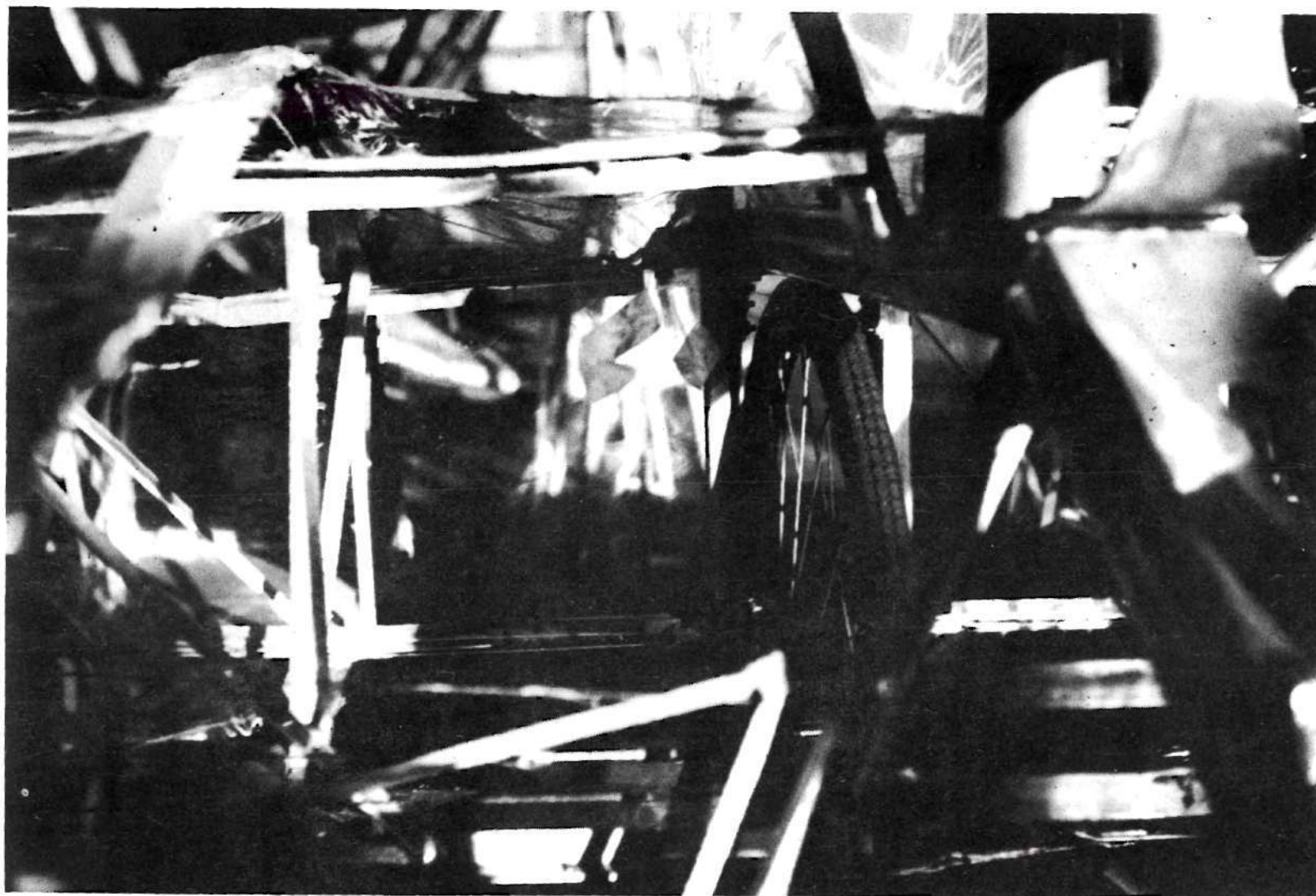


Fig. 12b Front View of Buckled Spar Cap

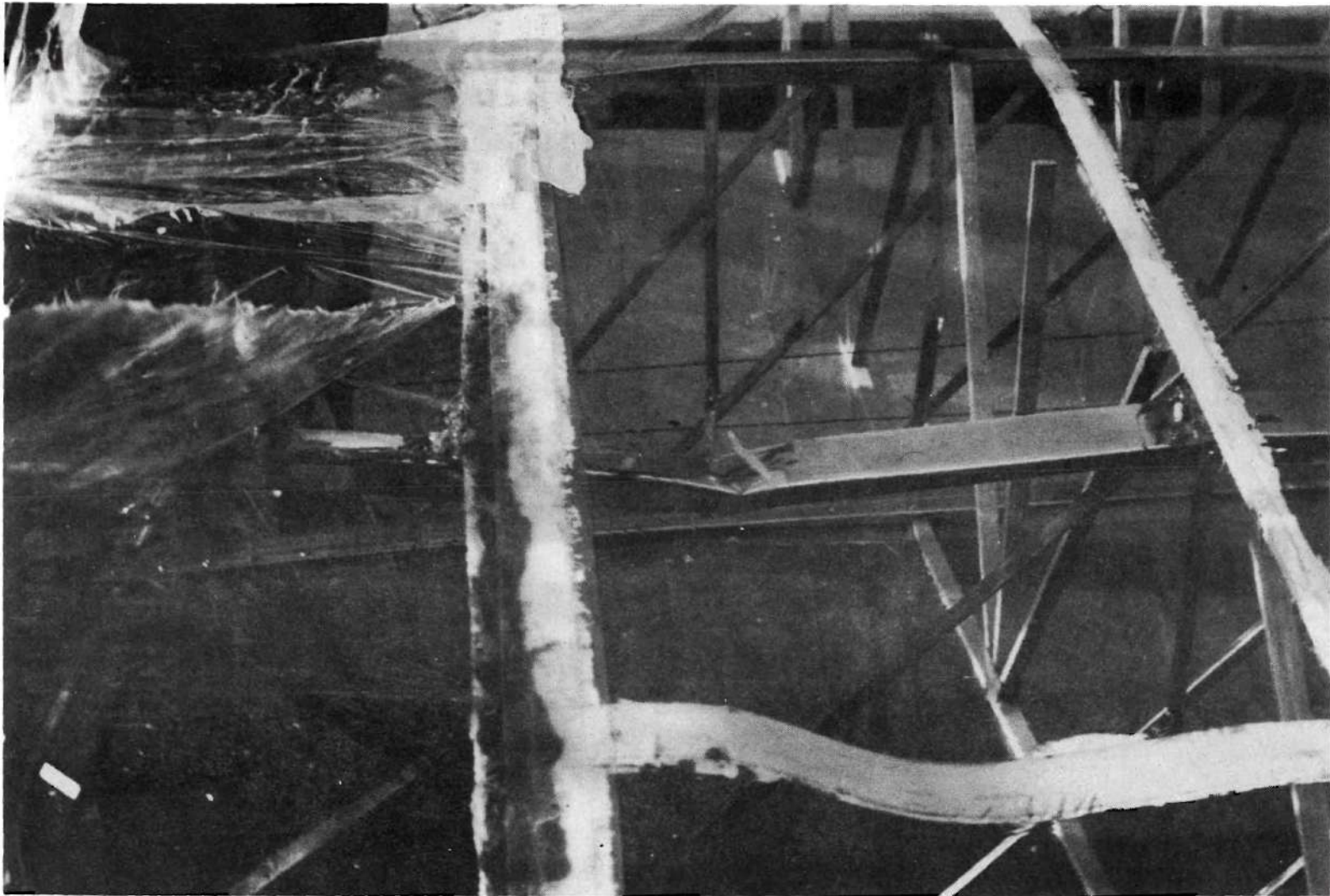


Fig. 12c Rear View of Buckled Spar Cap

APPENDIX VI

ESTIMATION OF AIRCRAFT PROFILE DRAG COEFFICIENT

The aircraft drag for all components except the wing was computed using experimental values from reference 2. The wing drag was read from Figure 10 to be $C_{D_{ow}} = 0.008$.

Fuselage Drag Coefficient

Wetted area of tailcone	43 sq. ft.
Wetted area of cockpit	102 sq. ft.
<hr/>	
Total wetted area of fuselage	145 sq. ft.
Fuselage R_n	2,670,000
C_{D_f}	0.0032
$\Delta C_{D_{of}}$	0.00114

Tip Plates

Wetted area	24 ft. ²
$C_{D_{TP}}$	0.0095
$\Delta C_{D_{oTP}}$	0.0008

Interference

Area of wing section joining fuselage	11.5 sq. ft.
$C_{D_{int}}$	0.004
$\Delta C_{D_{oint}}$	0.0002

Shroud

The velocity used to find the dynamic pressure of the shroud was

taken as one-half the sum of the velocities over the inner and outer surfaces of the shroud.

Wetted area	45.3 sq. ft.
q	1.25 psf.
C_{Ds}	0.009
$\Delta C_{D_{os}}$	0.0016

Resultant Profile Drag Coefficient

The total profile drag is the sum of the coefficients found above.

$$C_{Do} = 0.012$$

APPENDIX VII

SHROUD AND PROPELLER DESIGN

It is desirable to have a highly efficient propulsion system for the man-powered airplane, and in order to obtain high efficiency the propeller losses must be made as small as possible. The shrouded counter-rotation propellers greatly reduce two types of losses, the blade tip and wake rotational losses. Under the design conditions of the MPA it is doubtful if the blade tip loss prevented by the shroud is significant in view of the additional drag imposed on the system by the added wetted surface of the shroud. However, since the propellers counter rotate, there is no external torque on the system, thus the need for a large vertical stabilizer is eliminated. By incorporating the rudder and elevator controls into the trailing edge of the shroud, the need for further stabilizer surfaces was eliminated. Thus, the shroud was obtained with very little addition of wetted area over that of a conventional tail configuration, resulting in an overall increase in efficiency of the propulsion system. Also, the drag losses are reduced when the lift to drag ratio is high for the airfoil of the propeller.

Basically, the propeller design procedure uses a combination of the momentum and thin airfoil theories, while the shroud design procedure is the determination of a mean camber line which, with the propeller, will satisfy the conditions of the ultimate wake (momentum theory) at the trailing edge plane (or disk) of the shroud.

Propeller Design Procedure

The desired ideal efficiency of the propellers is assumed (94 per cent), and the thrust required and flight velocity are known from performance calculations.

Thus, the axial induced velocity of the ultimate wake is found

$$\delta = \frac{2}{\eta_p} V (1 - \eta_p) \quad (\text{reference 4})$$

The most efficient propeller is one which causes the wake to move as a solid body. The induced velocity found above is constant across any plane parallel to the propeller disk, which means that the wake does move as a solid body.

The volume flow is found by finding the mass flow and dividing by density. The mass flow can be determined, since the thrust is equal to the mass flow times the change in velocity of the flow, i.e. the mass flow equals the thrust divided by the total induced velocity. Now with the mass flow known, the radius of the ultimate wake can be found along with the total axial velocity through the propeller disk (accounting for the reduction in area due to the propeller hub).

The blade bound vortex strength is found once the rotational velocity of the propeller (n), and the number of blades (b) are determined.

$$b \Gamma = \frac{(1 - \eta_p^2) V^2}{n \eta_p} \quad (\text{reference 4})$$

The resultant velocity (U) at a blade element is then found from the vector addition of the axial velocity, the tangential velocity, and

the induced velocity due to the blade's bound vortex system.

Then, if the blade chord distribution is assumed, the blade lift distribution is determined

$$cC_l = \frac{2b}{bV} \quad (\text{reference 4})$$

The chord was chosen to be constant (6 inches) along the blades.

The angle between the resultant flow at a given section and the propeller disk is equal to the inverse tangent of the axial velocity divided by the total tangential flow at the section. The total blade station angle of attack is found by adding to this angle the additional amount required by the airfoil to produce the section lift coefficient found from the above formula.

Table 1

Propeller Section Data

r inches	ϕ		C_l	
	front	rear	front	rear
6.3	73°45"	65°45"	0.285	0.270
8.4	66°30"	61°09"	0.282	0.268
10.5	60°25"	56°25"	0.271	0.247
12.6	55°00"	52°09"	0.253	0.234
14.7	50°25"	48°08"	0.236	0.221
16.8	46°18"	44°35"	0.214	0.201
18.9	42°41"	41°23"	0.200	0.195
21.0	39°38"	38°32"	0.189	0.185
23.1	36°51"	36°00"	0.178	0.174
25.2	34°25"	33°42"	0.168	0.165
27.3	32°18"	31°40"	0.159	0.156
29.4	30°21"	29°51"	0.150	0.148
31.5	28°37"	28°12"	0.142	0.140
33.6	27°05"	26°44"	0.135	0.134
35.1	25°40"	25°22"	0.129	0.127
37.8	24°23"	24°09"	0.123	0.121
39.9	23°13"	23°03"	0.117	0.116
42.0	22°10"	22°00"	0.112	0.111

Shroud Design Procedure

The method of singularities was used to determine a shroud mean camber line that would cause conditions of the ultimate wake to be satisfied at the trailing edge of the shroud.

This was accomplished by replacing the trailing edge disk of the shroud by a sink with unit strength equal to the induced velocity of the ultimate wake, and assuming a mean camber line with a vortex distribution for the shroud. The stream (or volume flow) function is found for the contribution of the sink, vortex distribution, free-stream, and center-body (prop hub) at the shroud trailing edge. The value of the stream function thus found must be equal to the value from the ultimate wake data of the propeller. Setting the two quantities equal to each other determines the strengths of the vortex distribution.

Then the stream function can be found for several points on a radial line on the disks described by each annular vortex ring. A new position can be found for each vortex ring by satisfying the condition of continuity. Thus, a new shroud mean camber line is obtained. The process is repeated until satisfactory convergence is attained.

A thickness distribution is then superimposed on the above mean camber line that will satisfy the stream function at both the inner and outer surfaces.

Table 2

Shroud Mean Camber Line

Station ¹	Radial Position in Inches	Axial Position in Inches
1	42.0	0
2	42.1	6
3	42.3	12
4	42.5	18
5	43.1	24
6	43.4	30
7	43.7	36
8	43.9	42

¹Beginning at trailing edge proceeding forward to leading edge.

APPENDIX VIII

HORSEPOWER AVAILABLE

A dynamometer was built to determine the rate at which power could be generated and the endurance for a constant power output by a man. The dynamometer was built using a bicycle frame on which a fly-wheel with a high moment of inertia was mounted and driven by conventional bicycle pedals and chain. An adjustable brake was mounted on the hub of the wheel with a lever-arm extending out from the brake to a spring scale. The distance along the lever-arm from the center of the hub to the scale was such that when the pedals were turned at 60 rpm the scale read horsepower directly.

There is very little available information about the power output and endurance of man. This information would be very hard to correlate because of the great difference in the physical make-up between individuals. Due to the limited amount of time available, no extensive investigation was carried out to determine the power output and endurance in terms of physical make-up. However, the pilot was selected by taking the person (from several volunteers) who could, upon first trying, give the best power output and endurance (keeping in mind that such a person must be as light as possible for a given power output). A 160-pound man was selected to train as the pilot.

The next phase of the investigation was to determine an optimum pedal speed, i.e. a pedal speed that would give the best endurance for a constant power output.

It was determined that a rotational velocity of 60 rpm would be used with the length of the pedal arms adjusted to give the best pedal speed.

The conclusion drawn from these limited tests is that the pedal arms should be as long as the length of the legs will comfortably allow. Shortening the pedal arms and increasing the rotational velocity to maintain a given power output tends to sharply reduce the endurance of the man. Figure 13 shows the horsepower versus endurance of the pilot after two and one-half months of training for approximately 15 minutes per day on the dynamometer.

The moment of inertia of the fly-wheel was not sufficiently large to carry the wheel past the zero torque part of the pedal stroke (when the pedal arms are vertical) above the torque required for 0.75 horsepower. Further, the brake tended to grab above the torque required for 0.45 horsepower when the pedal arms were in the vertical position. This tended to tighten the pilot's leg muscles and shorten his endurance.

Due to the brevity of the training program and the difficulties encountered from the dynamometer, it is felt that the maximum power output and endurance could be improved under better circumstances.

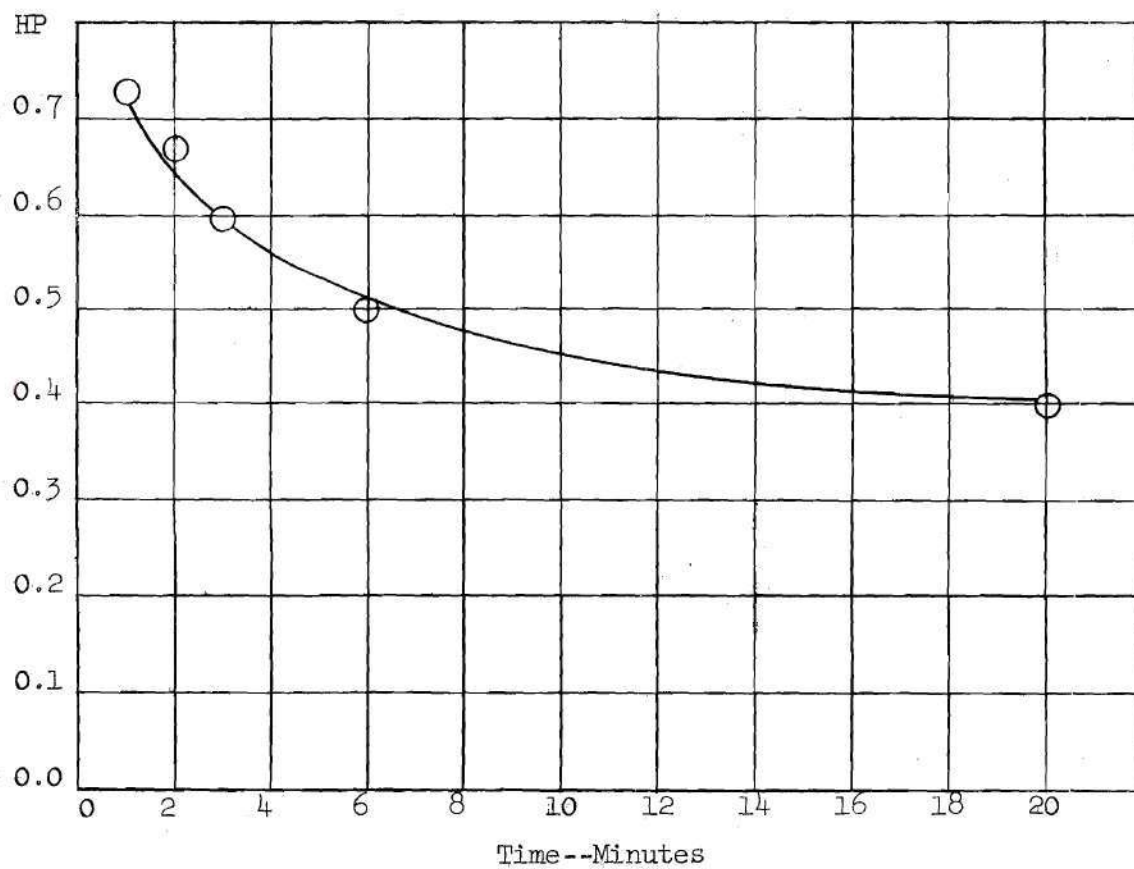


Fig. 13 Horsepower-Endurance Chart for a One Hundred and Sixty Pound Man